and TIMP-2 as described previously (Liang et al., 2006).

Real-time reverse transcriptase-polymerase chain reaction

Total RNA from the aortic arch was isolated using Trizol reagent (Invitrogen, Life Technologies, Inc., Carlsbad, CA) and then analyzed by real-time reverse transcriptase (RT)-polymerase chain reaction (PCR) (DNA Engine Opticon; MJ Research, Tokyo, Japan) (Liang et al., 2006). The RNA expression levels of MMP-1, -2, -3, -9, -12, -13, MT1-MMP, TIMP-1, -2, -3, and MCP-1 were evaluated using SYBR® Premix Ex TaqTM kits (Takara Bio Inc., Tokyo) according to the manufacturer's instructions. The panel of primers used for these analyses is shown in Table. 2. Each RNA quantity was normalized by the endogenous GAPDH control (Sun et al., 2005).

Western blot analysis

Fresh aortic specimens were collected and homogenized in ice-cold suspension buffer (10 mM Tris-HCL, pH 7.6, 100 mM NaCl) supplemented with a proteinase inhibitor cocktail (Sigma, St. Louis, MO) as described previously (Fan et al., 2004). The supernatant was collected and the protein content was measured using a Bio-Rad protein assay kit. Equal amounts of protein (10 μg) were loaded in each lane and separated by 10% SDS-PAGE. The proteins were transferred to pure nitrocellulose membranes (Bio-Rad). The membranes were incubated at 4°C overnight in the presence of each Ab (Liang et al., 2006), and then washed three times with 0.1% Tween 20 in PBS and stained with horseradish peroxidase-conjugated secondary Abs. The ECL system (Amersham Life Science, Buckinghamshire, UK) was used for detection with an LAS-1000 plus gel documentation system (Fujifilm, Tokyo, Japan).

In situ zymography

To localize the cellular site of MMP enzymatic activity in the lesions, liquid nitrogen-frozen specimens of aortas were embedded in Tissue-Tek OCT compound (Sakura Finetek Japan Co., Tokyo). Cryostat sections (8 μm thick) were made and mounted onto slides coated with a resorufin-labeled casein, a substrate for stromelysin and metalloelastase (EMD Biosciences, Inc., La Jolla, CA). The slides with sections were immediately placed in a moisture chamber at 37°C for 48 hours using the method as described by others (Galis et al., 1995b). The proteolytic areas of the sections were examined under a fluorescent microscope. To validate the specific nature of the casein breakdown by MMPs, control slides were pre-treated with Tris-buffer containing 10mM 10-phenanthroline, a specific inhibitor of MMP enzymatic activity (Molecular Probes, Eugene, OR).

Table 1. Clinical data of autopsy cases used for the current study

No.	Age	Sex	Clinical diagnosis
1	78	F	Interstitial pneumonia
2	80	F	Pneumonia + Pulmonary edema
3	77	M	Acute myocardial infarction
4	84	M	Acute myocardial infarction
5	61	M	Pancreatic head carcinoma
6	72	M	Malignant lymphoma
7	55	M	Acute myocardial infarction

All autopsies were performed at the Department of Pathology, School of Med, University of Occupational and Environmental Health. Aortas were collected during the autopsy and they were used for the analysis of mRNA expression by real-time RT-PCR.

MMP expression of U937-derived macrophages

To investigate the expression of different MMPs in macrophages stimulated by various cytokines, human U937 cells were differentiated into macrophages by incubation with 50 ng/ml PMA for 3 days. U937-derived macrophages were incubated in a serum-free medium in the presence of the following cytokines for 48h: MCP-1 (200 ng/ml), IL-6 (50 ng/ml), IL-10 (100 ng/ml), TNF-α (100 ng/ml), and GM-CSF (150 ng/ml). The optimal doses were selected according to the previous study (Wu et al., 2000). The conditioned media were collected for Western blotting and gelatin zymography and cellular mRNA was extracted for real-time RT-PCR and Western blotting.

Statistical analysis

All values were expressed as mean ± SEM and statistical significance was determined using Mann-Whitney's U-test for nonparametric analysis. Student's *t*-test was used to compare the result of other assays. In all cases, statistical significance was set at $P< 0.05$.

Results

Histological features of atherosclerotic lesions of rabbits

Through manipulation of the cholesterol content in the diet and the length of feeding, we were able to obtain different degrees of aortic atherosclerotic lesions from cholesterol-fed rabbits. We selected three time points to collect rabbit aortas. Rabbits fed a cholesterol diet for 6 wks developed very tiny fatty dots on the surface of the aorta (Fig. 1A). These lesions were basically composed of a single layer or a few layers of macrophages on the intima, representing the earliest events in the arterial intima during the pathogenesis of atherosclerosis in experimental animals (Watanabe et al., 1985). For the convenience of description, we defined these lesions as

early stage lesions. Accumulation of foam cells in the subendothelial space was consistently observed and became prominent after rabbits were fed a cholesterol diet for 12 wks or 16 wks. At these stages, in addition to the accumulation of foam cells, many smooth muscle cells along with extracellular matrix were intermingled

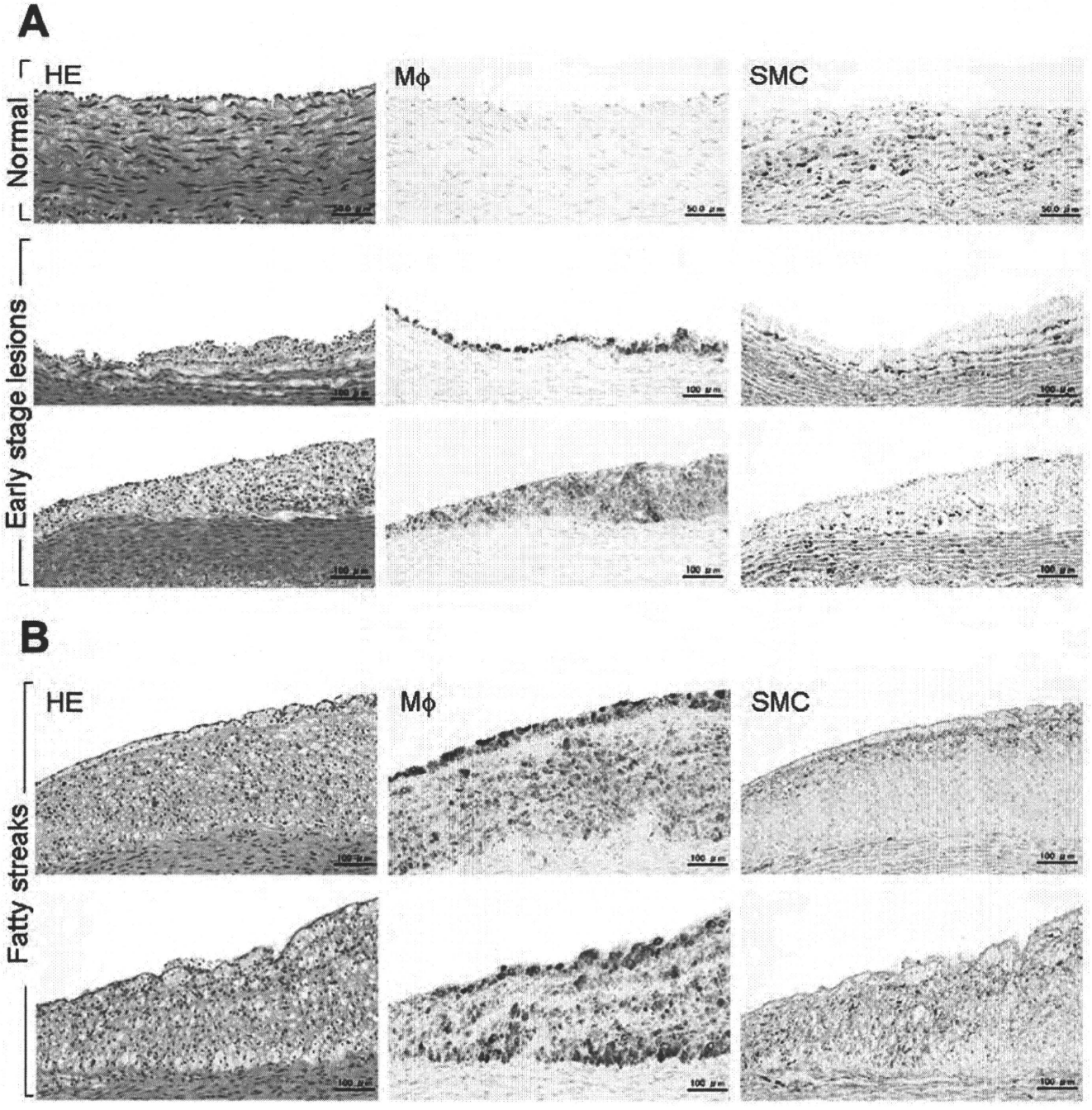

Fig. 1. Representative micrographs of early-stage lesions and fatty streaks in cholesterol-fed rabbits. **A.** Serial paraffin sections of the aorta of normal rabbits (top panel) and rabbits fed cholesterol for 6 wks (middle and bottom panels) were stained with either H&E or mAbs against macrophages (Møs) and smooth muscle cells (SMCs). The lesions are composed of a single or several layers of Møs and a few SMCs in cholesterol-fed rabbits. These lesions are designated "early-stage lesions". **B.** The fatty streaks of aortas from rabbits fed a cholesterol diet for 12 wks. Compared to the early-stage lesions above, the lesions become larger and contain many Møs intermingled with SMCs, either on the lesion surface (top), or throughout the lesions (bottom). These lesions are similar or equivalent to those of fatty streaks and preatheromas (types II and III lesions) in humans.

as the lesions progressed (Fig. 1B). These lesions are similar or equivalent to those of fatty streaks or preatheromas (types II and III lesions) in humans (Stary et al., 1995).

In WHHL rabbits at the ages of 24-wks, the lesions were composed of lipid cores and thick fibrous caps, while accumulation of macrophages was focally present (Fig. 2). These lesions mimic human advanced lesions of fibroatheroma and complicated lesions (types V and VI lesions) (Stary et al., 1995).

MMP and TIMP expression in the lesions of rabbits

We first characterized the mRNA expression profiles

Table 2. Primers for real-time RT-PCR.

Gene	Sequence	Product (bp)	TA (°C)	Accession #
Human MMP-1	(F) CTGGGAGCAAACACATCTGA; (R) CTGCTTGACCCTCAGAGACC	149	58.5	NM_002421
Human MMP-2	(F) ACGACCGCGACAAGAAGTAT; (R) ATTTGTTGCCCAGGAAAGTG	111	56.3	NM_004530
Human MMP-3	(F) GAGGACACCAGCATGAACCT; (R) TCACCTCCAATCCAAGGAAC	148	57.0	NM_002422
Human MMP-9	(F) TTGACAGCGACAAGAAGTGG; (R) CCCTCAGTGAAGCGGTACAT	148	57.0	NM_004994
Human MMP-12	(F) CCCGATCTCCATCATTTCAG; (R) TCACGGTTCATGTCAGGTGT	101	56.3	NM_002426
Human MMP-13	(F) TTGAGCTGGACTCATTGTCG; (R) CGCGAGATTTGTAGGATGGT	126	56.3	NM_002427
Human MT1-MMP (MMP-14)	(F) TGCCCAATGGAAAGACCTAC; (R) TGAATGACCCTCTGGGAGAC	138	57.0	U41078
Human TIMP-1	(F) ACATCCGGTTCGTCTACACC; (R) TGATGTGCAAGAGTCCATCC	120	57.0	NM_003254
Human TIMP-2	(F) AAGCGGTCAGTGAGAAGGAA; (R) TCTCAGGCCCTTTGAACATC	108	56.3	NM_003255
Human TIMP-3	(F) CCTGCTACTACCTGCCTTGC; (R) GGCGTAGTGTTTGGACTGGT	104	58.5	NM_000362
Human MCP-1	(F) AGCAAGTGTCCCAAAGAAGC; (R) GAGTTTGGGTTTGCTTGTCC	121	56.3	S71513
Human GAPDH	(F) CAATGACCCCTTCATTGACCTC; (R) AGCATCGCCCCACTTGATT	172	60.9	BC029340
Rabbit MMP-1	(F) TTCCAAAGCAGAGAGGCAAT; (R) GGAGTGAGGACGAACTGAGC	160	59.0	M17820
Rabbit MMP-2	(F) GGCATTCAAGAGCTCTACGG; (R) CCTGTGTGCAGATCTCAGGA	103	59.0	D63579
Rabbit MMP-3	(F) CGTTCCTGATGTTGGTCACTTC; (R) TTGGCAGATCCGGTGTGTAA	101	57.5	M25664
Rabbit MMP-9	(F) TGAGCTTTGACATCCTGCAC; (R) AAGAAAGGCGAGGAGAGAGG	186	53.0	D26514
Rabbit MMP-12	(F) TGAAGCGTGAGGATGTTGAG; (R) AAAGCATGGGCTATGACACC	181	59.0	AB006779
Rabbit MMP-13	(F) GGAGAGGCAGCAGTCTCCAG; (R) CCTCGGACAAATCATCATCC	135	59.0	AF059201
Rabbit MT1-MMP (MMP-14)	(F) TGCCCAATGGAAAGACCTAC; (R) GCCTTCCCACACTTTGATGT	110	56.3	U83918
Rabbit TIMP-1	(F) GGTTCCCTGGAACAGTCTGA; (R) GGTCTGTCCACAAGCAATGA	143	57.4	AY829730
Rabbit TIMP-2	(F) GCACATCACGCTCTGTGACT; (R) CCGGAGAGGAGATGTAGCAC	143	59.4	AF069713
Rabbit TIMP-3	(F) CTACTACCTGCCCTGCTTCG; (R) GGCGTAGTGTTTGGACTGGT	100	59.4	AF069714
Rabbit MCP-1	(F) AGCACCAAGTGTCCCAAAGA; (R) TGTGTTCTTGGGTTGTGGAA	163	60.0	M57440
Rabbit GAPDH	(F) ATCACTGCCACCCAGAAGAC; (R) GTGAGTTTCCCGTTCAGCTC	146	58.3	L23961

TA, annealing temperature

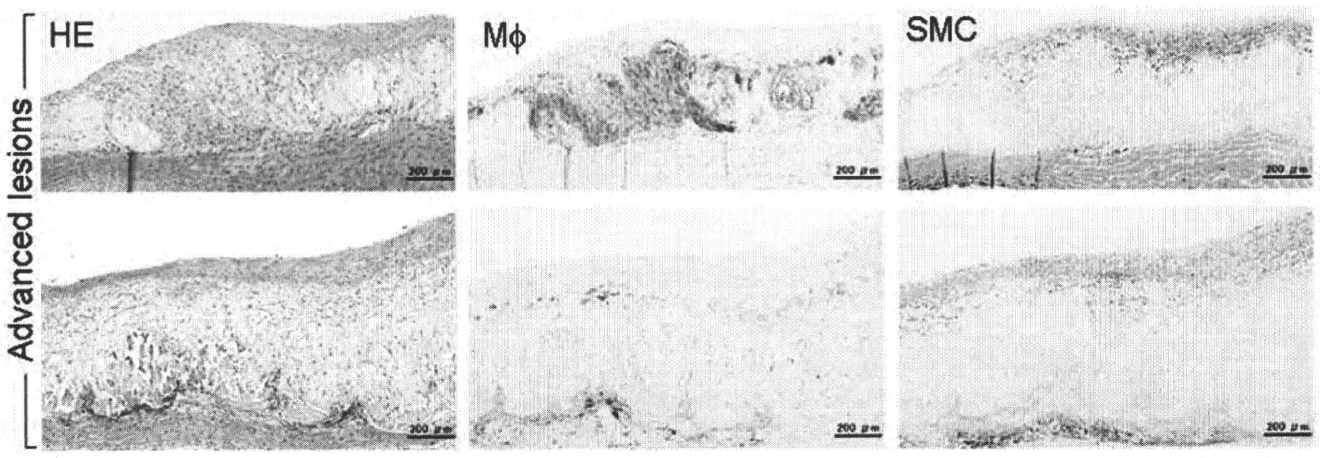

Fig. 2. Representative micrographs of advanced lesions of WHHL rabbits at 24 wks old. The lesions are characterized by the presence of a fibrous cap on the surface and lipid or necrotic cores, in which either Møs (top) or necrotic materials and calcium deposition (bottom), are present. SMCs are contained in the fibrous cap. These lesions mimic human advanced lesions ("fibroatheroma") and complicated lesions (types V and VI lesions).

of MMPs and TIMPs that have been detected in the lesions (Newby, 2005). By real-time RT-PCR analysis, we found that there were three distinct expression patterns with regard to changes in these MMPs. As shown in Fig.3A, the mRNA expression of MMP-1, -12, and -13 was barely detectable in the normal aorta. Once the lesions formed, the expression of these MMPs was evident, and it increased as the lesion progressed: starting from the early-stage lesions (6 wks) to fatty streaks (12 and 16 wks) of cholesterol diet-fed rabbits and WHHL rabbits at age 24-wks. Interestingly, increased expression of these MMPs was simultaneously associated with high expression of MCP-1 in the lesions (Fig. 3B, bottom panel). Immunohistochemical staining showed that macrophages were the major cellular sources of MMP-1 and -12 proteins in both early lesions and fatty streaks (Fig. 4A,B).

The second pattern of MMP expression was seen for MMP-3 and MT1-MMP (Fig. 3B, top and middle panels). Although their expression was normally present in the normal aorta (a pattern which clearly differed from those of MMP-1, -12, and -13), expression levels were markedly upregulated as the lesions progressed to the fatty streaks (in cholesterol-fed rabbits at 12 and 16 wks) and advanced lesions (in WHHL rabbits at 24 wks) compared to the normal aorta.

The third expression pattern in the lesions was that of gelatinases A and B (MMP-2 and MMP-9). The expression of both MMPs was detected in the normal aortas; however, their expression was not significantly changed, regardless of the presence or absence of the lesions, although MMP-2 expression was slightly elevated in the lesions of fatty streaks of 16-wk-cholesterol-fed rabbits (Fig. 3C). Immunohistochemical staining showed that MMP-2 proteins were faintly stained in intimal smooth muscle cells (Fig. 4B), and MMP-9 showed the same staining pattern (data not shown).

Finally, we examined the expression of TIMP family members in the lesions (Fig. 3D). Although all TIMPs were present in the normal arterial wall, TIMP-1 and -2 appeared to be increased in the fatty streaks, but TIMP-3 was not changed throughout. Immunohistochemical staining revealed that TIMP-2 was mainly expressed by intimal macrophages (data not shown).

To evaluate the expression of MMP proteins in the lesions, we also performed Western blotting analysis. Consistent with the findings of real-time RT-PCR,

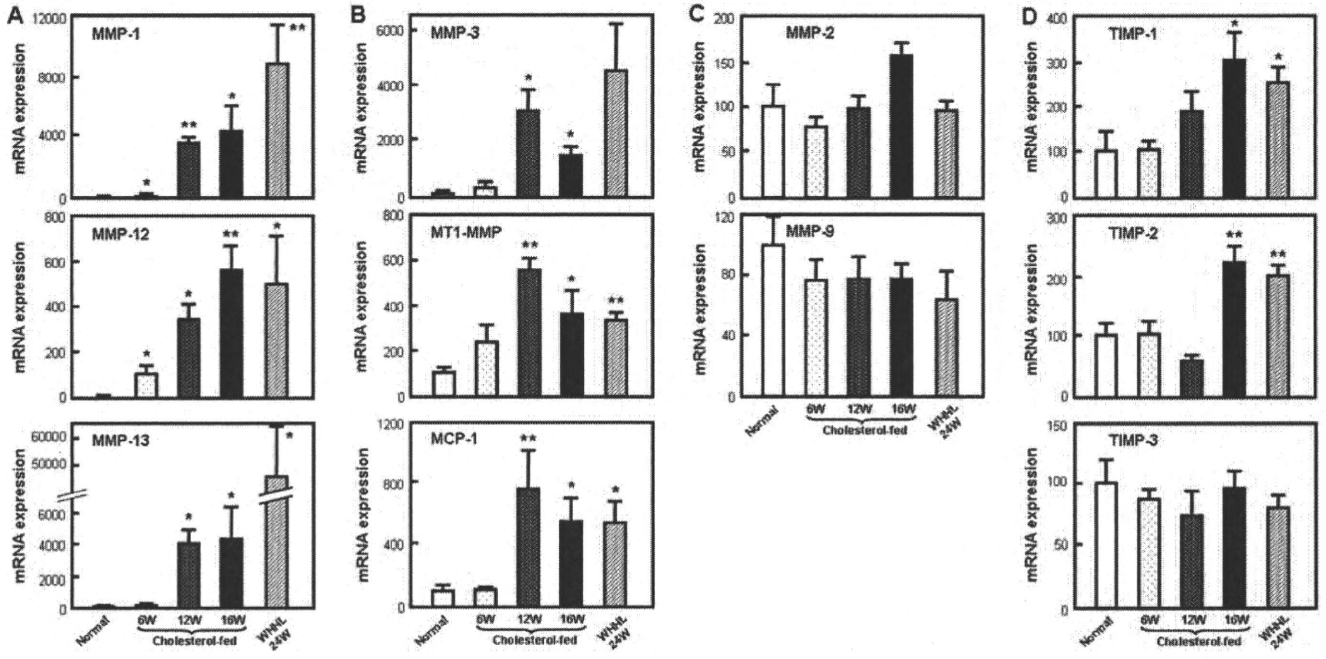

Fig. 3. MMP and TIMP gene expression in various lesions of cholesterol-fed and WHHL rabbits. The mRNA expression of each MMP and TIMP was analyzed by real-time RT-PCR as described in Materials and Methods, and expressed as a percentage of the control of normal rabbits. Each sample was analyzed in triplicate and data are expressed as the mean ± SEM. N=3 to 6 for each group. *P<0.05, **P<0.01 vs normal aortas. Expression patterns of MMP were arbitrarily classified into three categories: Pattern A is characterized by no expression in normal aorta, but markedly increased expression, including MMP-1, -12, and -13 expression in the lesions **(A)**. Pattern B includes MMP-3 and MT1-MMP, which are normally present in the aorta but are significantly increased with the progression of the lesions **(B)**. Both patterns A and B were accompanied by the simultaneous increase of a chemokine, monocyte chemoattractant protein-1 (MCP-1) (B, at the bottom). Pattern C includes the expression of gelatinases A and B (MMP-2 and MMP-9) **(C)**. Both were expressed in the normal aorta; however, their expression was not significantly affected by the presence of the lesions. Expression changes of TIMPs are shown in **D**.

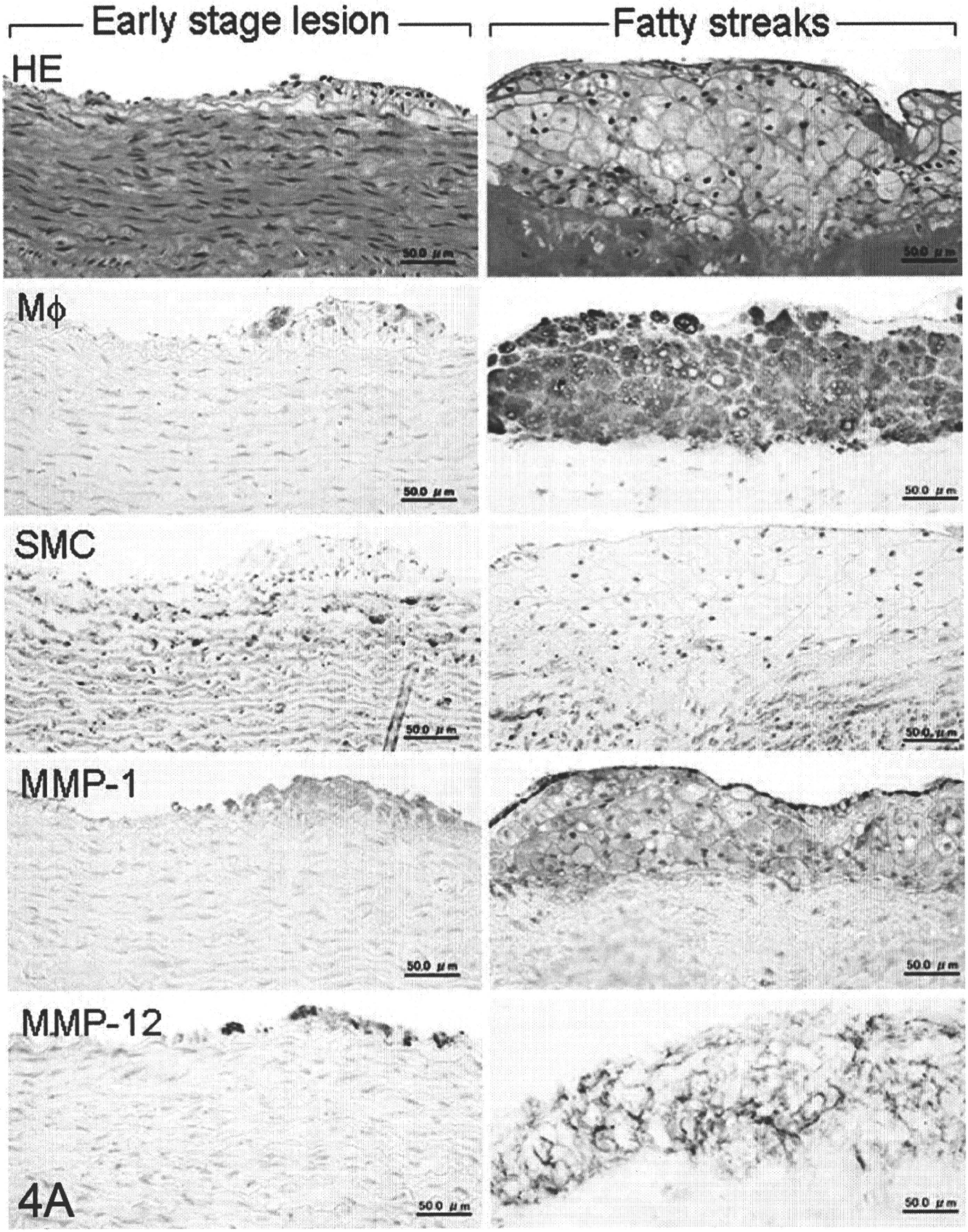
Early stage lesion
Fatty streaks
HE
Mϕ
SMC
MMP-1
MMP-12
4A
50.0 μm

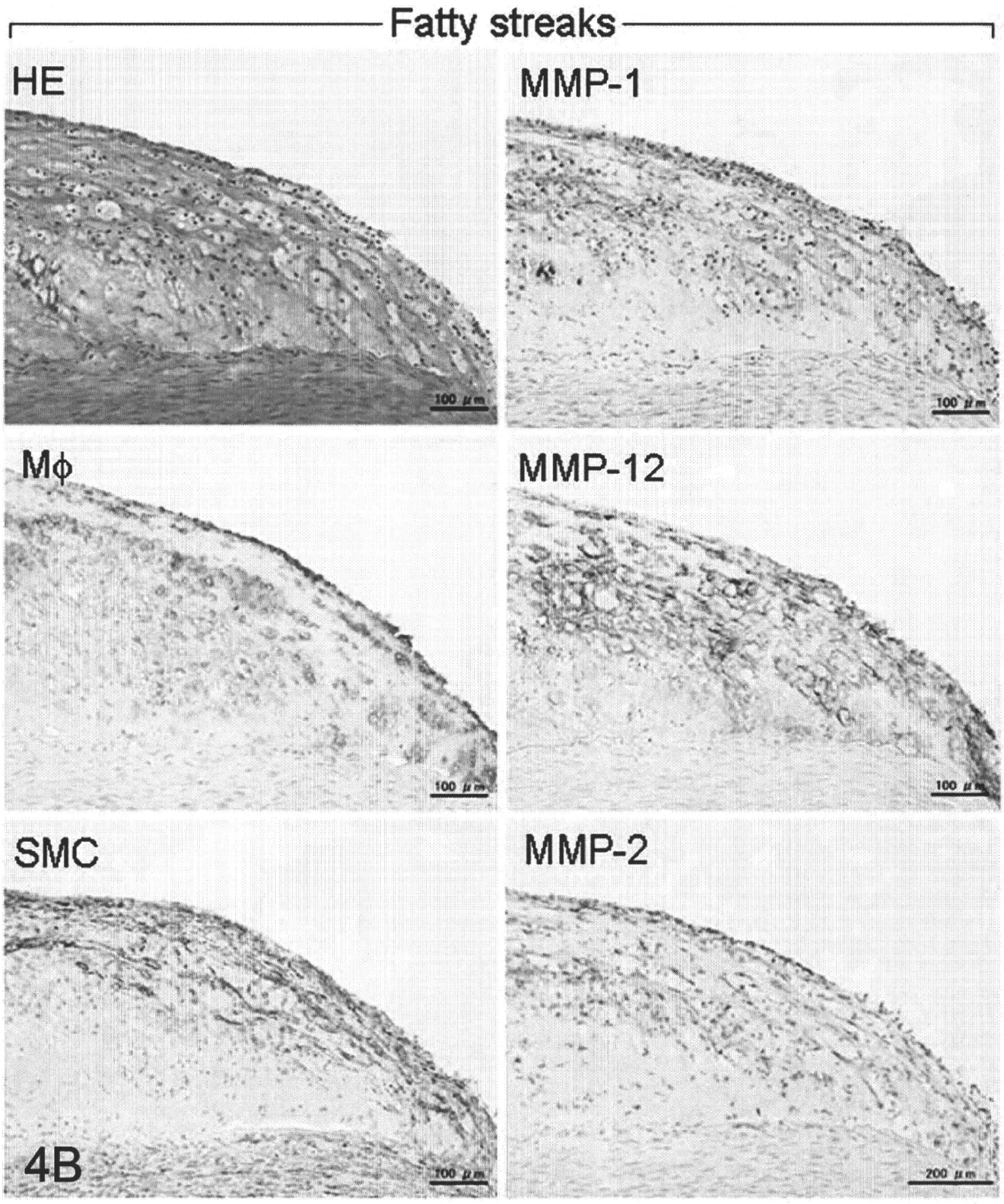

Fig. 4. Immunohistochemical demonstration of MMPs in the lesions of cholesterol-fed rabbits **(A, B). A.** Serial paraffin sections of lesions were stained with H&E or immunostained with each mAb. Immunoreactive proteins of MMP-1 and -12 are present in the early stage lesions (left) and fatty streaks (right) and they are closely associated with macrophage-derived foam cells. **B.** In another lesional area of fatty streaks where smooth muscle cells and extracellular matrix were increased (compared to the lesions above), MMP-1 and MMP-12 were also colocalized with macrophages, but MMP-2 was colocalized with smooth muscle cells.

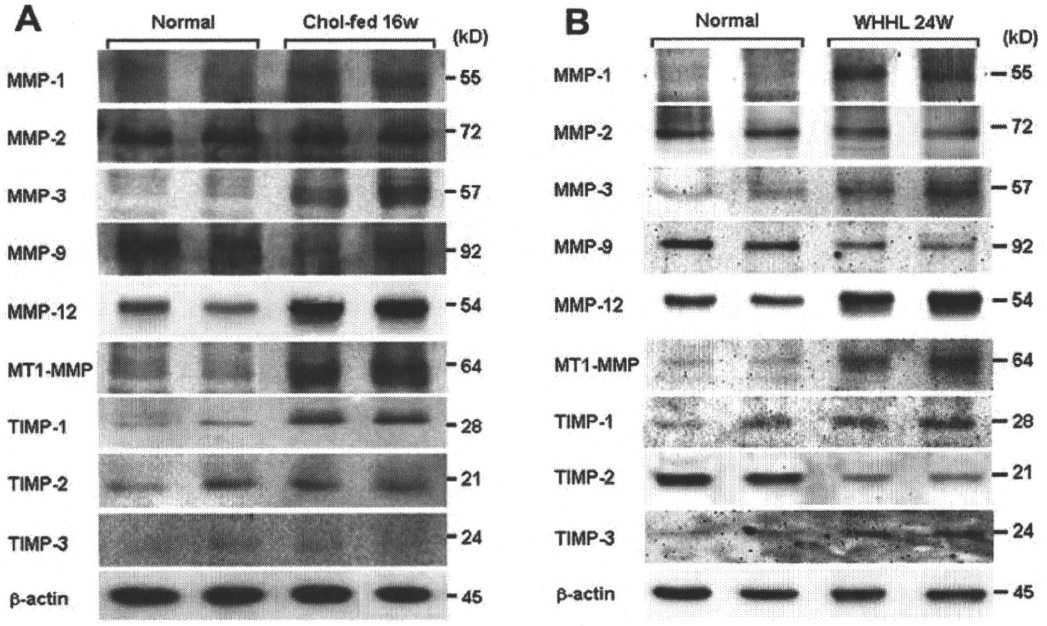

Fig. 5. Western blotting analysis of MMPs and TIMPs in the lesions. Total proteins isolated from aortas of normal rabbits and 16-wk-cholesterol-fed rabbits **(A)** and 24-wks WHHL rabbits **(B)** were fractionated by 10% SDS-PAGE, followed by immunoblotting using each Ab as described in Materials and Methods. Molecular size is shown on the right. ß-actin proteins are shown at the bottom to indicate that equal amounts of proteins were loaded in each lane. Compared to normal aortas, MMP-1, -3, -12, MT1-MMP, and TIMP-1 were increased, whereas MMP-2 and -9 were either unchanged or slightly reduced. Representative data from three separate analyses are shown.

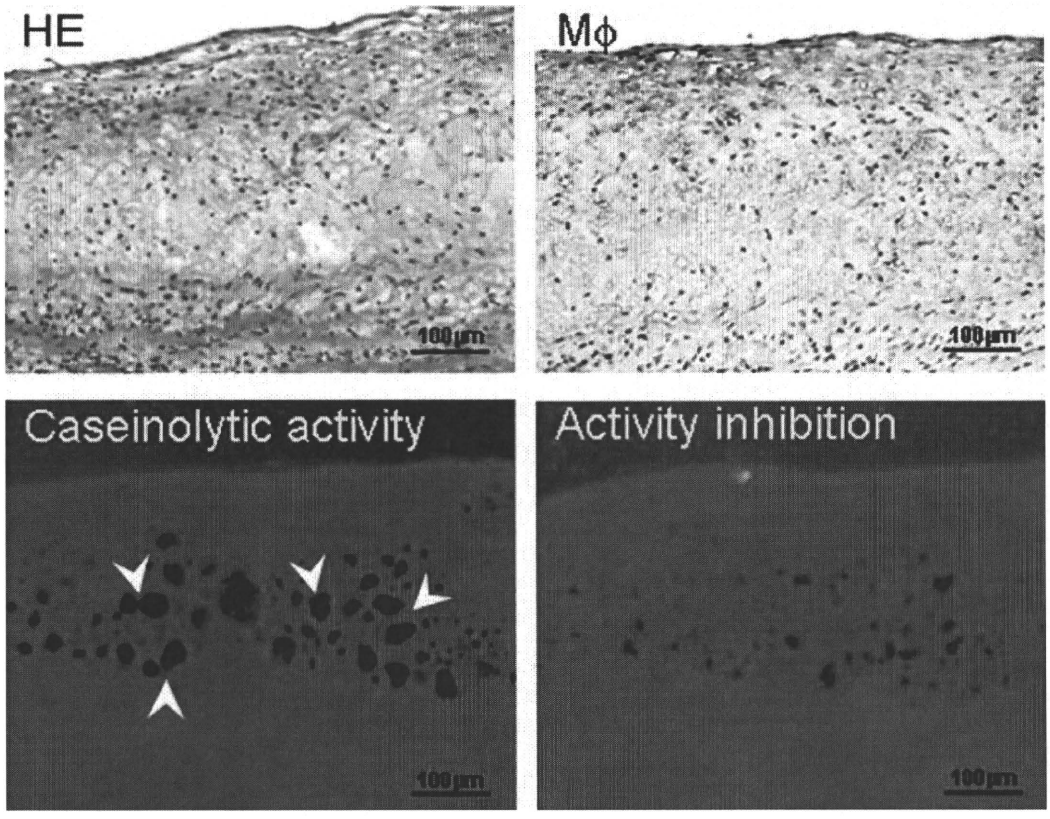

Fig. 6. *In situ* zymographic demonstration of MMP enzymatic activity in the lesions. *In situ* zymography was performed using cryostat sections of aortic arch of cholesterol-fed rabbits. The lesions are composed of many foam cells, as shown in H&E and immunohisto-chemical staining of macrophages (Møs) (upper panel). Caseinolytic activity was characterized by fluorescent substrate degradation (black areas indicated by white arrow heads), which can be dramatically inhibited by incubation with MMP inhibitor (bottom panel).

MMP-1 and MMP-3 proteins were almost totally undetectable, but pro-type MMP-12 proteins were faintly detected in the normal aorta (Fig. 5A). In spite of this, their protein expression, along with that of MT1-MMP and TIMP-1, was markedly increased in fatty streaks of cholesterol-fed rabbits (Fig. 5A) and advanced lesions of WHHL rabbits (Fig. 5B). MMP-2 and TIMP-3 protein expression patterns were the same as their mRNA expression patterns, while MMP-9 was reduced as the lesions progressed.

To localize the site of MMPs enzymatic activity in the lesions we performed in situ zymography. As shown in Fig.6, the casienolytic activity in the lesions can be visualized (arrow heads) and overlapped with macrophages, suggesting that macrophages are the major cells that produce MMP activity in the lesions.

MMP expression in human atherosclerotic lesions

Since the lesions of rabbits may not completely mirror those seen in humans, we compared the MMP expression patterns of rabbits with those of human specimens. Increased expression tendency of MMP-1, -12, -13, -2, -3, along with MCP-1, were almost identical to those of rabbits (although not statistically significant), while MT1-MMP tended to be decreased (Fig. 7). In

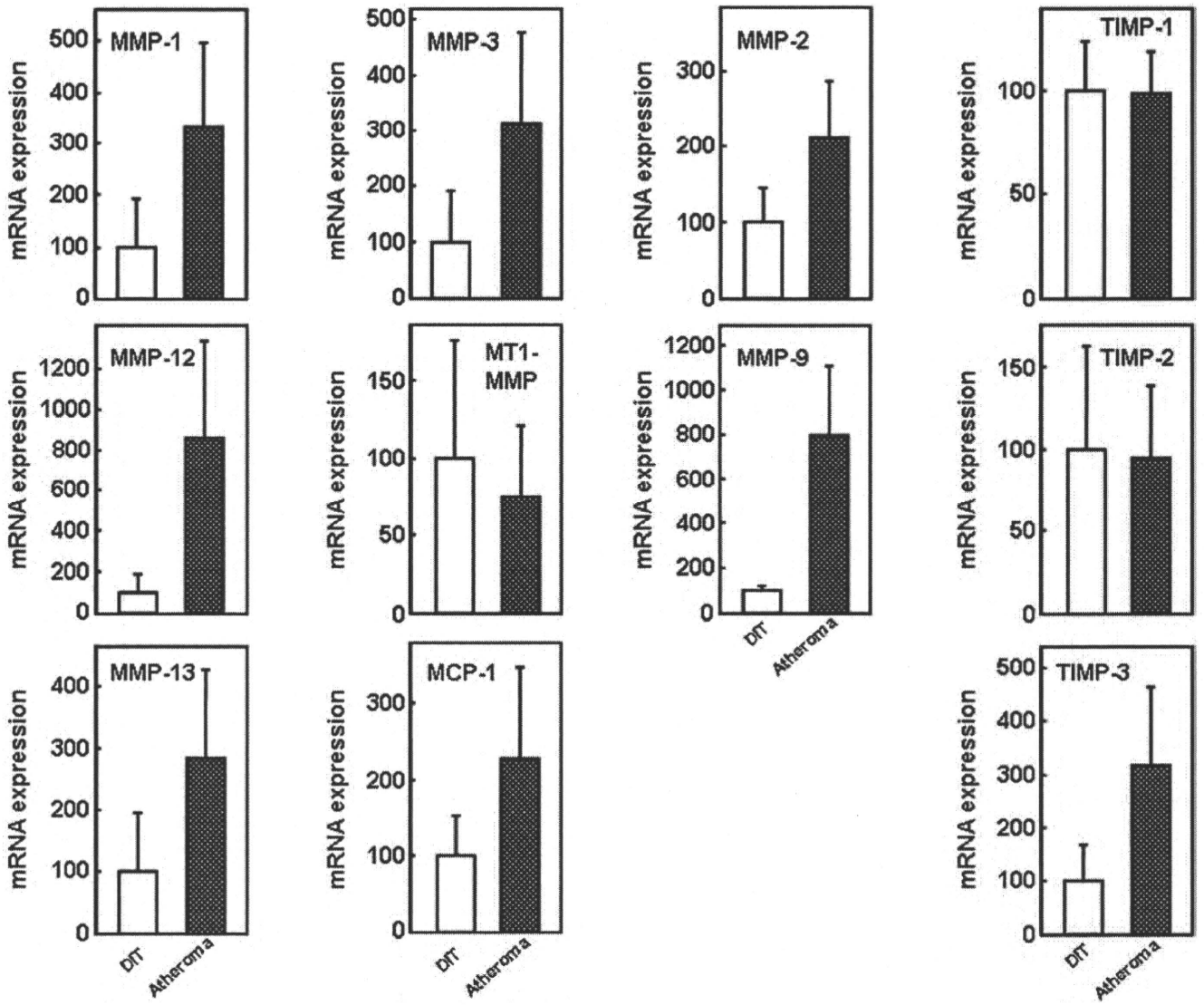

Fig. 7. MMP and TIMP expression profiling in the lesions of humans. mRNA expression of each MMP and TIMP was analyzed by real-time RT-PCR, as described in Materials and Methods. The samples were collected from 7 autopsy cases shown in Table 1, and grossly classified into normal-appearance (diffuse intimal thickening, DIT) and atheroma (fibrous plaques). Each sample was analyzed in triplicate and data are expressed as the mean ± SEM. N=7 for each group.

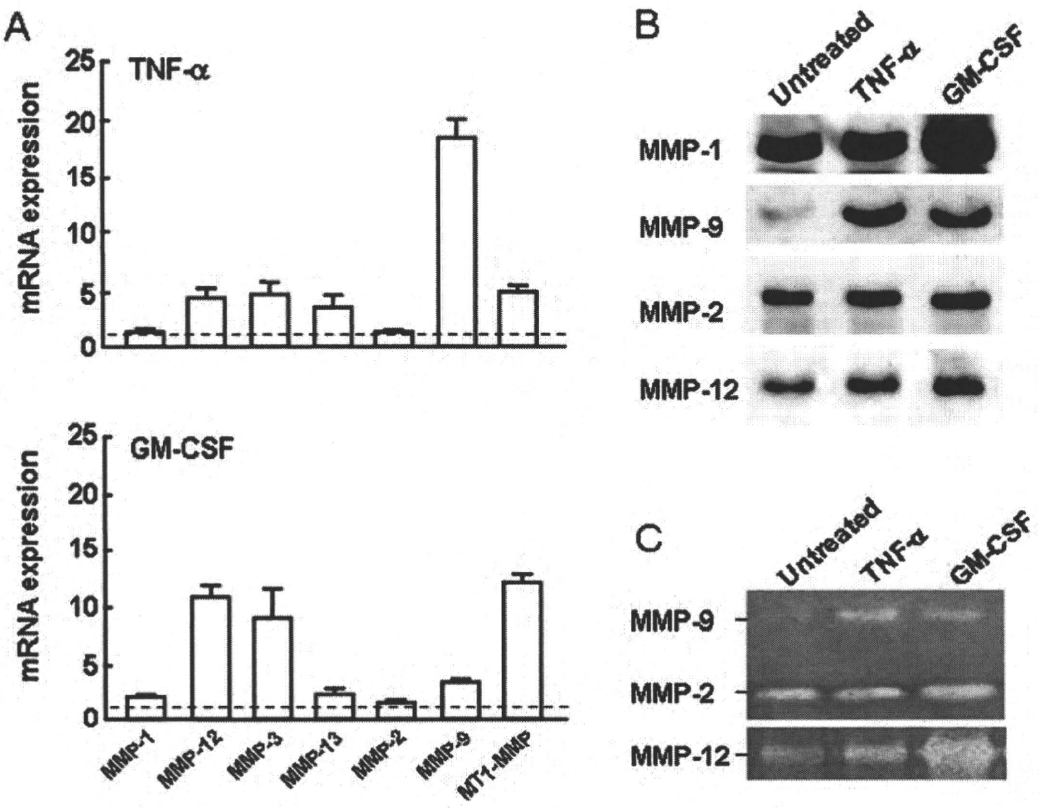

Fig. 8. MMP expression in U937-derived macrophages U937-derived macrophages were incubated with either TNF-α or GM-CSF for 48h, then the cells were homogenized and RNA was analyzed for the expression of different MMPs **(A)**. The conditioned media were used for the analyses of proteins by Western blots **(B)** and gelatin and casein zymography **(C)** (Wu et al., 2000). Each experiment was performed at least twice and the values are the mean ± SEM of triplicate analyses. The dotted lines indicate the levels of each gene expression in the condition without cytokines (control level).

addition, MMP-9 was increased in the lesions compared to diffuse intimal thickening in human aortas (Fig. 7), which is different from those found in rabbit lesions. We next examined whether the expression of MMPs in macrophages could be induced by inflammatory cytokines, presumably present in the arterial milieu. Among these cytokines, GM-CSF and TNF-α were a potent stimulator for upregulation of many MMPs, including MMP-1, -12, -3, -13, -9 and MT1-MMP, whereas MMP-2 was unchanged (Fig. 8A). These changes were also shown in the Western blots and zymography (Fig. 8B,C). However, incubation with MCP-1, IL-6 and IL-10 did not lead to the upregulation of MMPs in macrophages (data not shown).

Discussion

In this study, we demonstrated for the first time that the expression patterns of MMPs and TIMPs varied dependent upon the lesion progression. First, we found that MMP-1, -12, and -13 expression (barely present in the normal aortas) was markedly increased as the lesion appeared and progressed in both rabbit and human atherosclerotic lesions. This result suggests that these three MMPs are either associated with, or directly participate in, the lesion formation or stability by facilitating SMC entry. Because macrophages are the major cellular components in the early-stage lesions, it is very likely that the increased expression of these MMPs was caused by increased intimal macrophages in the lesions (Galis et al., 1995a). As many cytokines (e.g. GM-CSF and TNF-α) are virtually present in the lesions, upregulation of these MMPs derived from macrophages may be mediated through both autocrine and paracrine mechanism. In addition, enhanced accumulation of macrophages in the lesions driven by MCP-1 may lead to the vicious circle of the MMP upregulation and macrophage recruitment as the lesions progressed.

The functional roles of MMP-1, -12, and -13 in lesion formation are not completely clear, but enhanced enzymatic activity of MMP-12 in the intima may result in the excessive degradation of the basement membrane and elastic lamina, which subsequently facilitates lesion expansion through increased macrophage and smooth muscle migration and proliferation. This notion has been supported by recent studies using both MMP-12 transgenic rabbits and KO mice. Increased expression of MMP-12 in macrophages accelerates the progression of aortic and coronary atherosclerosis in transgenic rabbits (Liang et al., 2006), whereas deficiency of MMP-12 in apoE KO mice results in a reduction of the lesion size and buried fibrous layers of the branchiocephalic arteries (Johnson et al., 2005). The functional role of MMP-1 in atherosclerosis is not fully understood yet. In the current

study, we found that MMP-1 immunoreactive proteins are indeed present in human fatty streaks and unstable coronary plaques (data not shown). Because this enzyme is not normally present in mice, it is impossible to investigate its functional phenotype in KO mice (Vincenti et al., 1998). Instead, transgenic mice expressing human MMP-1 were created by Lemaitre and coworkers (Lemaitre et al., 2001). Their studies showed that increased MMP-1 expression in macrophages of apoE KO mice led to a reduction of aortic atherosclerosis, suggesting that MMP-1 may play an atheroprotective role (Lemaitre et al., 2001). It seems that MMP-13 deficiency in apoE KO mice did not affect the lesion growth either, although collagen accumulation was enhanced (Deguchi et al., 2005). Despite these observations, further studies will be required to clarify the physiological functions of MMP-1 and -13 in the pathogenesis of atherosclerosis (Vincenti et al., 1998).

In addition to MMP-1, 12, and -13, we found that MMP-3 and MT1-MMP (also called MMP-14) were upregulated in rabbits, but MT1-MMP was not changed in human atherosclerotic lesions. However, both of these MMPs were present in normal arteries, suggesting that they are essential for maintaining normal arterial remodeling and functions. Silence and coworkers reported that MMP-3 deficiency in apoE KO mice fed a cholesterol-rich diet for 30 wks increased the thoracic aortic lesion size (Silence et al., 2001) but it is not known whether MMP-3 deficiency affects early-stage lesion formation. MT1-MMP has been implicated in the lesions of human atherosclerotic lesions, but its precise functions have not been examined. MT1-MMP KO mice were developed (Atkinson et al., 2005) and it has been shown that MT1-MMP has a significant role in smooth muscle cell migration (Filippov et al., 2005).

In contrast to the above MMPs (which were upregulated in the lesions), MMP-2 and -9 were normally expressed in the arterial wall but remained unchanged (both mRNA and protein levels) regardless of the presence of the lesion progression in rabbits. This result observed in rabbits was surprising and unexpected because such an expression pattern in rabbits is apparently different from that of human atherosclerotic lesions, in which MMP-9 tended to be upregulated. This discrepancy between rabbit and human MMP-9 expression suggests that there is a species difference between the nature of atherosclerotic lesions and/or macrophage protease repertoire. This difference was also seen in the expression of TIMPs of the lesions: upregulation of TIMP-1 and -2 in rabbits, yet upregulation of TIMP-3 in humans. MMP-2 and MMP-9 are physiologically essential for arterial remodeling in the tunica media, by mediating smooth muscle cell migration (Galis et al., 2002; Kuzuya et al., 2003). The low expression of MMP-9 in rabbits may help explain why the advanced lesions of coronary arteries in WHHL rabbits were seldom ruptured (Shiomi et al., 2003a). It was reported that MMP-9 was not significantly changed in apoE KO mice fed a high fat diet for 16 wks (Jeng et al., 1999). On the other hand, it has been reported that MMP-2 and -9 are both required, and work in concert to produce aortic aneurysms (Longo et al., 2002) and protect against the lesion formation in apoE KO mice (Luttun et al., 2004; Kuzuya et al., 2006). Recently, Gough et al. reported that macrophage-specific expression of the active form of MMP-9 led to the rupture of aortic plaques in apoE KO mice (Gough et al., 2006).

In the current study, we also characterized the expression patterns of TIMPs and showed that TIMP-1 and -2 were upregulated as the lesions advanced in rabbits. This finding is also consistent with the study by Zaltsman et al., who demonstrated increased secretion of TIMP-1 and -2 from the aorta explants of cholesterol-fed rabbits by zymography (Zaltsman et al., 1999). Therefore, TIMP-1 and -2 may be the major endogenous inhibitors that counterbalance increased MMP activity in the lesions, although this hypothesis remains unverified.

In conclusion, we have demonstrated for the first time that MMPs, along with their inhibitors, are differentially upregulated in the different types of atherosclerotic lesions of both rabbits and humans. Although further studies are still needed to clarify the functional roles played by each of the MMPs and TIMPs during lesion formation, our results may provide important clues for the development of MMP inhibitors in the future. Because the currently available synthetic MMP inhibitors suffer from lack of specificity, poor oral bioavailability, and strong unrelated side-effects, the development of effective and specific MMP inhibitors is essential. Our data also suggests that atherosclerotic lesions are different in terms of MMPs expression between rabbits and humans, therefore care should be taken for testing specific MMPs inhibitors when using animal models.

References

Atkinson J.J., Holmbeck K., Yamada S., Birkedal-Hansen H., Parks W.C. and Senior R.M. (2005). Membrane-type 1 matrix metalloproteinase is required for normal alveolar development. Dev. Dyn. 232, 1079-1090.

Brown D.L., Desai K.K., Vakili B.A., Nouneh C., Lee H.M. and Golub L.M. (2004). Clinical and biochemical results of the metalloproteinase inhibition with subantimicrobial doses of doxycycline to prevent acute coronary syndromes (MIDAS) pilot trial. Arterioscler. Thromb. Vasc. Biol. 24, 733-738.

Curci J.A., Liao S., Huffman M.D., Shapiro S.D. and Thompson R.W. (1998). Expression and localization of macrophage elastase (matrix metalloproteinase-12) in abdominal aortic aneurysms. J. Clin. Invest. 102, 1900-1910.

Deguchi J.O., Aikawa E., Libby P., Vachon J.R., Inada M., Krane S.M., Whittaker P. and Aikawa M. (2005). Matrix metalloproteinase-13/collagenase-3 deletion promotes collagen accumulation and organization in mouse atherosclerotic plaques. Circulation 112, 2708-2715.

Fan J., Wang X., Wu L., Matsumoto S.I., Liang J., Koike T., Ichikawa T., Sun H., Shikama H., Sasaguri Y. and Watanabe T. (2004).

Macrophage-specific overexpression of human matrix metalloproteinase-12 in transgenic rabbits. Transgenic Res. 13, 261-269.

Filippov S., Koenig G.C., Chun T.H., Hotary K.B., Ota I., Bugge T.H., Roberts J.D., Fay W.P., Birkedal-Hansen H., Holmbeck K., Sabeh F., Allen E.D. and Weiss S.J. (2005). MT1-matrix metalloproteinase directs arterial wall invasion and neointima formation by vascular smooth muscle cells. J. Exp. Med. 202, 663-671.

Galis Z.S. and Khatri J.J. (2002). Matrix metalloproteinases in vascular remodeling and atherogenesis: the good, the bad, and the ugly. Circ. Res. 90, 251-262.

Galis Z.S., Sukhova G.K., Lark M.W. and Libby P. (1994). Increased expression of matrix metalloproteinases and matrix degrading activity in vulnerable regions of human atherosclerotic plaques. J. Clin. Invest. 94, 2493-2503.

Galis Z.S., Sukhova G.K., Kranzhofer R., Clark S. and Libby P. (1995a). Macrophage foam cells from experimental atheroma constitutively produce matrix-degrading proteinases. Proc. Natl. Acad. Sci. USA 92, 402-406.

Galis Z.S., Sukhova G.K. and Libby P. (1995b). Microscopic localization of active proteases by in situ zymography: detection of matrix metalloproteinase activity in vascular tissue. FASEB J. 9, 974-980.

Galis Z.S., Johnson C., Godin D., Magid R., Shipley J.M., Senior R.M. and Ivan E. (2002). Targeted disruption of the matrix metalloproteinase-9 gene impairs smooth muscle cell migration and geometrical arterial remodeling. Circ. Res. 91, 852-859.

Gough P.J., Gomez I.G., Wille P.T. and Raines E.W. (2006). Macrophage expression of active MMP-9 induces acute plaque disruption in apoE-deficient mice. J. Clin. Invest. 116, 59-69.

Halpert I., Sires U.I., Roby J.D., Potter-Perigo S., Wight T.N., Shapiro S.D., Welgus H.G., Wickline S.A. and Parks W.C. (1996). Matrilysin is expressed by lipid-laden macrophages at sites of potential rupture in atherosclerotic lesions and localizes to areas of versican deposition, a proteoglycan substrate for the enzyme. Proc. Natl. Acad. Sci. USA 93, 9748-9753.

Henney A.M., Wakeley P.R., Davies M.J., Foster K., Hembry R., Murphy G. and Humphries S. (1991). Localization of stromelysin gene expression in atherosclerotic plaques by in situ hybridization. Proc. Natl. Acad. Sci. USA 88, 8154-8158.

Herman M.P., Sukhova G.K., Libby P., Gerdes N., Tang N., Horton D.B., Kilbride M., Breitbart R.E., Chun M. and Schonbeck U. (2001). Expression of neutrophil collagenase (matrix metalloproteinase-8) in human atheroma: a novel collagenolytic pathway suggested by transcriptional profiling. Circulation 104, 1899-1904.

Jeng A.Y., Chou M., Sawyer W.K., Caplan S.L., Von Linden-Reed J., Jeune M. and Prescott M.F. (1999). Enhanced expression of matrix metalloproteinase-3, -12, and -13 mRNAs in the aortas of apolipoprotein E-deficient mice with advanced atherosclerosis. Ann. NY Acad. Sci. 878, 555-558.

Johnson J.L., Fritsche-Danielson R., Behrendt M., Westin-Eriksson A., Wennbo H., Herslof M., Elebring M., George S.J., McPheat W.L. and Jackson C.L. (2006). Effect of broad-spectrum matrix metalloproteinase inhibition on atherosclerotic plaque stability. Cardiovasc. Res. 71, 586-595.

Johnson J.L., George S.J., Newby A.C. and Jackson C.L. (2005). Divergent effects of matrix metalloproteinases 3, 7, 9, and 12 on atherosclerotic plaque stability in mouse brachiocephalic arteries. Proc. Natl. Acad. Sci. USA 102, 15575-15580.

Kuzuya M., Kanda S., Sasaki T., Tamaya-Mori N., Cheng X.W., Itoh T., Itohara S. and Iguchi A. (2003). Deficiency of gelatinase a suppresses smooth muscle cell invasion and development of experimental intimal hyperplasia. Circulation 108, 1375-1381.

Kuzuya M., Nakamura K., Sasaki T., Cheng X.W., Itohara S. and Iguchi A. (2006). Effect of MMP-2 deficiency on atherosclerotic lesion formation in apoE-deficient mice. Arterioscler. Thromb. Vasc. Biol. 26, 1120-1125.

Lemaitre V. and D'Armiento J. (2006). Matrix metalloproteinases in development and disease. Birth Defects. Res. C. Embryo. Today 78, 1-10.

Lemaitre V., O'Byrne T.K., Borczuk A.C., Okada Y., Tall A.R. and D'Armiento J. (2001). ApoE knockout mice expressing human matrix metalloproteinase-1 in macrophages have less advanced atherosclerosis. J. Clin. Invest. 107, 1227-1234.

Liang J., Liu E., Yu Y., Kitajima S., Koike T., Jin Y., Morimoto M., Hatakeyama K., Asada Y., Watanabe T., Sasaguri Y., Watanabe S. and Fan J. (2006). Macrophage metalloelastase accelerates the progression of atherosclerosis in transgenic rabbits. Circulation 113, 1993-2001.

Longo G.M., Xiong W., Greiner T.C., Zhao Y., Fiotti N. and Baxter B.T. (2002). Matrix metalloproteinases 2 and 9 work in concert to produce aortic aneurysms. J. Clin. Invest. 110, 625-632.

Luttun A., Lutgens E., Manderveld A., Maris K., Collen D., Carmeliet P. and Moons L. (2004). Loss of matrix metalloproteinase-9 or matrix metalloproteinase-12 protects apolipoprotein E-deficient mice against atherosclerotic media destruction but differentially affects plaque growth. Circulation 109, 1408-1414.

Manning M.W., Cassis L.A. and Daugherty A. (2003). Differential effects of doxycycline, a broad-spectrum matrix metalloproteinase inhibitor, on angiotensin II-induced atherosclerosis and abdominal aortic aneurysms. Arterioscler. Thromb. Vasc. Biol. 23, 483-488.

Newby A.C. (2005). Dual role of matrix metalloproteinases (matrixins) in intimal thickening and atherosclerotic plaque rupture. Physiol. Rev. 85, 1-31.

Newman K.M., Jean-Claude J., Li H., Scholes J.V., Ogata Y., Nagase H. and Tilson M. D. (1994). Cellular localization of matrix metalloproteinases in the abdominal aortic aneurysm wall. J. Vasc. Surg. 20, 814-820.

Rajavashisth T.B., Xu X.P., Jovinge S., Meisel S., Xu X.O., Chai N.N., Fishbein M.C., Kaul S., Cercek B., Sharifi B. and Shah P.K. (1999). Membrane type 1 matrix metalloproteinase expression in human atherosclerotic plaques: evidence for activation by proinflammatory mediators. Circulation 99, 3103-3109.

Schonbeck U., Mach F., Sukhova G.K., Atkinson E., Levesque E., Herman M., Graber P., Basset P. and Libby P. (1999). Expression of stromelysin-3 in atherosclerotic lesions: regulation via CD40-CD40 ligand signaling in vitro and in vivo. J. Exp. Med. 189, 843-853.

Shiomi M., Ito T., Yamada S., Kawashima S. and Fan J. (2003). Development of an animal model for spontaneous myocardial infarction (WHHLMI rabbit). Arterioscler. Thromb. Vasc. Biol. 23, 1239-1244.

Silence J., Lupu F., Collen D. and Lijnen H.R. (2001). Persistence of atherosclerotic plaque but reduced aneurysm formation in mice with stromelysin-1 (MMP-3) gene inactivation. Arterioscler. Thromb. Vasc. Biol. 21, 1440-1445.

Stary H.C., Chandler A.B., Dinsmore R.E., Fuster V., Glagov S., Insull W. Jr, Rosenfeld M.E., Schwartz C.J., Wagner W.D. and Wissler R.W. (1995). A definition of advanced types of atherosclerotic lesions and a histological classification of atherosclerosis. A report

from the Committee on Vascular Lesions of the Council on Arteriosclerosis, American Heart Association. Circulation 92, 1355-1374.

Sukhova G.K., Schonbeck U., Rabkin E., Schoen F.J., Poole A.R., Billinghurst R.C. and Libby P. (1999). Evidence for increased collagenolysis by interstitial collagenases-1 and -3 in vulnerable human atheromatous plaques. Circulation 99, 2503-2509.

Sun H., Koike T., Ichikawa T., Hatakeyama K., Shiomi M., Zhang B., Kitajima S., Morimoto M., Watanabe T., Asada Y., Chen Y.E. and Fan J. (2005). C-reactive protein in atherosclerotic lesions: its origin and pathophysiological significance. Am. J. Pathol. 167, 1139-1148.

Uzui H., Harpf A., Liu M., Doherty T.M., Shukla A., Chai N.N., Tripathi P.V., Jovinge S., Wilkin D.J., Asotra K., Shah P.K. and Rajavashisth T.B. (2002). Increased expression of membrane type 3-matrix metalloproteinase in human atherosclerotic plaque: role of activated macrophages and inflammatory cytokines. Circulation 106, 3024-3030.

Vincenti M.P., Coon C.I., Mengshol J.A., Yocum S., Mitchell P. and Brinckerhoff C.E. (1998). Cloning of the gene for interstitial collagenase-3 (matrix metalloproteinase-13) from rabbit synovial fibroblasts: differential expression with collagenase-1 (matrix metalloproteinase-1). Biochem. J. 331 (Pt 1), 341-346.

Visse R. and Nagase H. (2003). Matrix metalloproteinases and tissue inhibitors of metalloproteinases: structure, function, and biochemistry. Circ. Res. 92, 827-839.

Watanabe T., Hirata M., Yoshikawa Y., Nagafuchi Y., Toyoshima H. and Watanabe T. (1985). Role of macrophages in atherosclerosis. Sequential observations of cholesterol-induced rabbit aortic lesion by the immunoperoxidase technique using monoclonal antimacrophage antibody. Lab. Invest. 53, 80-90.

Wu L., Fan J., Matsumoto S. and Watanabe T. (2000). Induction and regulation of matrix metalloproteinase-12 by cytokines and CD40 signaling in monocyte/macrophages. Biochem. Biophys. Res. Commun. 269, 808-815.

Zaltsman A.B., George S.J. and Newby A.C. (1999). Increased secretion of tissue inhibitors of metalloproteinases 1 and 2 from the aortas of cholesterol fed rabbits partially counterbalances increased metalloproteinase activity. Arterioscler. Thromb. Vasc. Biol. 19, 1700-1707.

Accepted July 14, 2008

The American Journal of Pathology, Vol. 172, No. 5, May 2008

DOI: 10.2353/ajpath.2008.070604

Vascular Biology, Atherosclerosis and Endothelium Biology

Matrix Metalloproteinase 12 Accelerates the Initiation of Atherosclerosis and Stimulates the Progression of Fatty Streaks to Fibrous Plaques in Transgenic Rabbits

Sohsuke Yamada,*† Ke-Yong Wang,* Akihide Tanimoto,* Jianglin Fan,‡ Shohei Shimajiri,* Shuji Kitajima,§ Masatoshi Morimoto,§ Masato Tsutsui,¶ Teruo Watanabe,§‖ Kosei Yasumoto,† and Yasuyuki Sasaguri*

From the Departments of Pathology and Cell Biology, Surgery,† and Pharmacology,¶ School of Medicine, University of Occupational and Environmental Health, Kitakyushu; the Department of Molecular Pathology,‡ Faculty of Medicine, University of Yamanashi, Yamanashi; the Analytical Research Center for Experimental Sciences,§ Saga University, Saga; and the Kyurin Omtest Laboratory Department,‖ Kyurin Corporation, Kitakyushu, Japan*

Whether fatty streaks are directly followed by fibrous plaque formation in atherosclerosis remains controversial. Disruption of the basement membrane and elastic layers is thought to be essential for this process. Matrix metalloproteinase 12 (MMP-12) can degrade a broad spectrum of substrates, but the role of MMP-12 in the early stage of atherosclerosis is unclear. To investigate MMP-12 function in the initiation and progression of atherosclerosis, we investigated macrophage migration and elastolysis in relation to fatty streaks in human MMP-12 transgenic (hMMP-12 Tg) rabbits. Fatty streaks in hMMP-12 Tg rabbits fed a 1% cholesterol diet for 6 weeks (cholesterol-induced model of atherosclerosis) were more pronounced and were associated with more significant degradation of the internal elastic layer compared with wild-type (WT) animals. Numbers of infiltrating macrophages and smooth muscle cells in the lesions were increased in hMMP-12 Tg compared with WT animals. In both cuff- and ligation-induced models of atherosclerosis, smooth muscle cell-predominant atherosclerotic lesions were elevated with significant elastolysis of the internal elastic lamina in Tg compared with WT animals; "microelastolytic sites" were recognized before formation of the neointima in the cuff model only. These results indicate that MMP-12 may be critical to the initiation and progression of atherosclerosis via degradation of the elastic layers and/or basement membrane. Therefore, a specific MMP-12 inhibitor might prove useful for the treatment of progressive atherosclerosis. ***(Am J Pathol 2008, 172:1419–1429; DOI: 10.2353/ajpath.2008.070604)***

In atherosclerosis, the extracellular matrix (ECM), mainly produced by smooth muscle cells (SMCs) of the synthetic phenotype in the arterial intima, includes collagen types I, III, IV, V, VIII, and laminin.[1–2] Collagen types I and III are synthesized and located in the intima and fibrous caps, and the shoulder regions of the plaque are rich in type I procollagen-synthesizing cells.[3] The basement membrane underlying the vascular endothelium is a complex structure that results from the interaction of laminin, entactin, and heparin sulfate proteoglycan along with type IV collagen.[4] Elastin is a main and critical component of the arterial media, and it maintains the wall structure and function by its elastic nature. In addition to elastin in the media, relatively large amounts of elastin are also synthesized by SMCs that become located in increasing number in the intima with the progression of atherosclerosis.[1,5]

We reported previously that matrix metalloproteinases (MMPs), which are a family of zinc-dependent proteinases, are synthesized and secreted by endothelial cells, SMCs, and macrophages and are involved in ECM turnover in relation to remodeling of the arterial wall.[6–9] Recently, a vast amount of knowledge about the roles of

Accepted for publication February 4, 2008.

Current address of T.W.: Department of Pathology, Fukuoka Wajiro Hospital, Fukuoka, Japan.

Address reprint requests to Yasuyuki Sasaguri, M.D., Ph.D., Department of Pathology and Cell Biology, School of Medicine, University of Occupational and Environmental Health, 1-1 Iseigaoka, Yahatanishi-ku, Kitakyushu 807-8555, Japan. E-mail: yasu3219@med.uoeh-u.ac.jp.

MMPs in atherosclerosis has accumulated, and more than 20 members of this family are currently known.[10–15] Several studies have revealed the following features of MMP-12 knockout mice: macrophages with a markedly diminished capacity to degrade ECM and an essential disability to penetrate reconstituted basement membranes,[16] a significant reduction in the number of infiltrating macrophages in allergen-induced lung inflammation relative to that in wild-type (WT) mice,[17] and reductions in atherosclerotic lesion size and macrophage number,[18] suggesting strongly that macrophage-mediated basement membrane proteolysis by MMP-12 is critically necessary for cell invasion at inflammatory sites.

First identified as a potent elastolytic metalloproteinase specially synthesized by macrophages, MMP-12 can degrade a broad spectrum of ECM components.[19,20] Therefore, human MMP-12 (hMMP-12) transgenic (Tg) rabbits, which specifically overexpress hMMP-12 in their tissue macrophages, were recently generated,[21] and these rabbits were shown to be useful for investigating the role of MMP-12 in arthritis.[22] The overexpression of macrophage-derived hMMP-12 was later shown to accelerate the degradation of the medial elastic laminae in advanced atherosclerosis and abdominal aortic aneurysms.[23] However, the role of MMP-12 in early atherosclerotic lesions was not conspicuous.

In humans, fatty streaks are thought to be a requisite event in the initiation of atherosclerosis, with additional factors needed for its progression. According to the compelling hypothesis known as the "response to injury theory,"[24] after immigration of monocytes/macrophages from the peripheral blood into the intima via degradation of the basement membrane, early atherosclerotic lesions (mainly fatty streaks) appear. Their appearance is followed by a microscopic event, ie, the migration of SMCs from the media to the intima, which probably results in the progression from fatty streaks to fibrous plaques. Considering this process, elastolysis of the internal elastic lamina would need to be accelerated for such a microscopic transition. In the current study, we investigated the details of elastolysis of the elastic layer over a relatively short period of time using hMMP-12 Tg rabbits in three different types of experimental models of atherosclerosis, ie, cholesterol induced, cuff induced, and ligation induced, and discussed the role of the disruption of the basement membrane and elastolysis of the internal elastic layer by MMP-12 in the early stage of atherosclerosis.

Materials and Methods

Experimental Designs

Three- or 4-month-old male hMMP-12 Tg and WT rabbits,[21] weighing approximately 1.5 to 2.0 kg, were divided into three groups. The first experimental group was fed a 1% cholesterol diet (120 g/day and water) to induce hypercholesterolemia, which was assessed by weekly measurement of plasma lipids (total cholesterol, triglycerides, high-density lipoproteins, and low-density lipoproteins). Every morning, we checked their meal boxes to ensure that the diet had been consumed and weekly measured their body weight. Then the animals were terminated by injection of an overdose of veterinary Ketaral^R and Domitor^R at 6 or 9 weeks and then autopsied. Rabbits with an extremely high or low cholesterol level were excluded from this experimental group.

The second and third experimental groups of rabbits were used to prepare femoral cuff-induced and carotid ligation-induced atherosclerosis models.[25] These rabbits were anesthetized with veterinary Ketaral^R and Domitor^R, and the bilateral femoral or lateral carotid arteries were cuffed by use of a polyethylene tube (inside diameter, 2.0 mm; outside diameter, 3.0 mm; Natsume Co., Tokyo, Japan) or ligated by silk sutures, respectively, as described previously.[25] The animals were terminated at 1 or 3 weeks by injection of an overdose of veterinary Ketaral^R and Domitor^R, and both cuffed femoral and ligated carotid arteries were excised. For excision, the bilateral femoral arteries were cut at both sides of the cuff point; and the lateral carotid arteries, close to the ligation point on one side and approximately 10 mm from it on the other side. All rabbits recovered and showed no symptoms of stroke. Arteries affected by significant artificial damage due to the surgical procedure were excluded from the study.

Animals

In this experiment, human MMP-12 (hMMP-12) transgenic (Tg) rabbits were used as the experimental animals[21]; and specific pathogen-free Japanese white rabbits (KBT Oriental Corporation, Saga, Japan) were used as the WT controls.

Immunohistochemistry

Immunohistochemical staining was performed using a Dako Envision kit (Dako Cytomation Co., Kyoto, Japan) according to the manufacturer's instructions. For this purpose, we used mouse monoclonal antibodies against smooth muscle actin (α-SMA; Dako Cytomation Co.), rabbit macrophages (RAM-11; Dako Cytomation Co.), and the hMMP-12 catalytic domain (MAB 919; R&D Systems, Minneapolis, MN), as reported previously.[23,25] The number of smooth muscle cells positive for α-SMA or of macrophages positive for RAM-11 was determined by counting 10 high-power fields limited to the atherosclerotic lesion thoroughly and equally from each aorta (fatty streaks in hypercholesterolemia model) or artery (neointima or adventitia in cuff- or ligation-induced injury model).

Quantitative Assessment of Cholesterol-, Cuff-, and Ligation-Induced Atherosclerosis

The aortas and arteries were removed and immediately immersed in cold PBS, fixed in 10% neutral buffered formalin, and embedded in paraffin for histological examination. Thick-paraffin sections (4 μm) were stained with hematoxylin and eosin (H&E) or elastica van Gieson (EVG) stains or by immunohistochemical techniques to

assess the degree of atherosclerosis and degradation of the elastic layers.[23,25] Twenty-six aortas from rabbits (n = 16 and 10 for hMMP-12 Tg and WT, respectively) fed the 1% cholesterol diet were opened longitudinally, pinned out flat on Styrofoam sheets, and stained with oil red O after having been fixed in 10% neutral buffered formalin for 24 hours. To measure atherosclerotic lesions, we photographed the whole aortas with an Olympus Camedia E-10 digital camera (Olympus Co., Tokyo, Japan). The red area relative to the whole surface area was measured by use of computerized NIH imaging software for rough estimation of the percentage of the total aortic area that was atherosclerotic. After the calculation, the preparations were cut into cross sections, in particular, at the marked atherosclerotic sites, for H&E, EVG, and immunohistochemical staining. Ten aortas (n = 5 for hMMP-12 Tg and n = 5 for WT) from animals fed the 1% cholesterol diet for 6 weeks, in which just early-stage atherosclerotic lesions (mainly fatty streaks) had formed in the thoracic aorta, were additionally examined by preparing up to 2500 sequential 4-μm cross sections to observe the details of elastolysis. Of each 10 serial sections, at least three sections were stained, either immunohistochemically or with H&E or EVG, to evaluate elastolysis in detail. In cuff- and ligation-induced models 1 and 3 weeks after the surgical treatment, the resected arteries (n = 30 and 32 for Tg and WT, respectively) were also cut into 4-μm cross sections to observe and evaluate atherosclerotic lesions microscopically.

For the quantitative analysis, after staining, these sequential slides were scanned at a resolution of 300 dpi in 24-bit full color by use of an Epson ES-8500 color image scanner (Epson Co., Tokyo) or were captured by a 600ES digital camera (Pixera, Los Gatos, CA) attached to an Olympus BX51 light microscope and measured with Studio 3.0 (Pixera) and NIH image for the evaluation of the intima-to-media ratio (I/M ratio) and elastolysis ratio.[23,24] For calculations of the I/M ratio, we measured the thickened intimal and normal medial areas of arteries; and for the elastolytic ratio, we measured the length of the elastolytic portions and of the whole internal elastic lamina in these serial sections.

Casein Zymography and mRNA Quantification

For zymography, 25 μg of protein extracts of the atherosclerotic aortas was mixed with SDS sample buffer without reducing agent and loaded onto a 10% SDS-polyacrylamide gel containing 0.2% casein, as described in detail previously.[21] Digestion bands were quantified using an image analyzer system (NIH image). Changes in the mRNA levels of MMPs in high-cholesterol diet-induced aortas, cuffed femoral arteries, or ligated carotid arteries were quantified by conducting the real-time RT-PCR on total RNA prepared with TRIzol reagent. The synthesized cDNA was quantified using TaqMan quantitative PCR analysis of each gene with the ABI PRISM 7700 Detection System (Applied Biosystems, Foster City, CA) according to the manufacturer's protocol. Specifically, primer and probe sequences used were as follows: for human MMP-12, 5′-AGCTCTCTGTGACCCCAATTTG (forward), 5′-AGCCAGAAGAACCTGTCTTTGAAG (reverse), and 5′-TTTGATGCT-GTCACTACCGTGGGAAATAAGAT-CT (probe); for rabbit MMP-12 (rMMP-12), 5′-AACGA-CCAGTGTCCGTTTAATTTC (forward), 5′-ACTTGATGTC-TGTCTCCAATTTCAT-AAG (reverse), and 5′-TGGCCA-ACCTTGCCTTCAGG (probe); for rabbit MMP-1, 5′-AAA-GATTTCAGAAATTACAACCTGTATCG (forward), 5′-TC-AAAGCCCCAA-TATCAGTAGAATG (reverse), and 5′-CTCATGAACTGGGCCATTCCCTTGG (probe); for rabbit MMP-2, 5′-TCACCTTCCTGGGCAACAAG (forward), 5′-GAGG-TCGCGCACCACATC (reverse), and 5′-CTGTAC-CAGCGCCGGCCGC (probe); for rabbit MMP-9, 5′-CC-CTGATAAAGGATACAGCCTGTT (forward), 5′-CCCCT-CTAG-GTAGCGGTACATG (reverse), and 5′-CATGCA-CTGGGCTTGGATCACTCCT (probe); and for rabbit glyceraldehyde-3-phosphate dehydrogenase, 5′-AGGGCG-GAGCCAAAAGG (forward), 5′-TTGCTGACAATC-TTGA-GAGAGTT-GTC (reverse), and 5′-ATGCCCCCATGT-TTGTGATGGGC (probe). Each RNA quantity was normalized to its respective glyceraldehyde-3-phosphate dehydrogenase mRNA quantity.

Statistical Analyses

All values were expressed as the mean ± SE, and statistical significance was analyzed using Student's t-test or the Mann-Whitney's U-test for nonparametric analysis. Statistical significance was set at $P < 0.05$.

Results

En Face and Cross-Section Analyses of Cholesterol-Induced Fatty Streaks in the Aortic Arch

As shown in Figure 1A, fatty streaks in the hMMP-12 Tg rabbit were grossly more evident in the aortic arch and in the upper portion of the thoracic aorta compared with those in the WT animals. In the thoracic aorta, WT animals showed a tendency for fatty streak distribution in the branches of the bronchial and intercostal artery branches. Fatty streaks in the hMMP-12 Tg animal, however, were relatively diffusely spread throughout the thoracic aorta compared with those in the WT rabbit.

Quantitative analysis of the whole aorta en face stained with oil red O showed that hMMP-12 Tg rabbits fed the 1% cholesterol diet developed more extensive atherosclerotic lesions than WT rabbits at 6 or 9 weeks (Figure 1A), and the difference was statistically noted at both times ($P < 0.05$; Figure 1B). Similar to those of the WT rabbits, the cholesterol levels of hMMP-12 Tg rabbits fed the high-cholesterol diet were increased up to 2000 mg/dl during the first 6 weeks (Figure 1C).

Similar to these gross findings, microscopic analysis of cross sections of the aortic arch and the upper portion of the thoracic aorta revealed that hMMP-12 Tg rabbits developed much more pronounced aortic atherosclero-

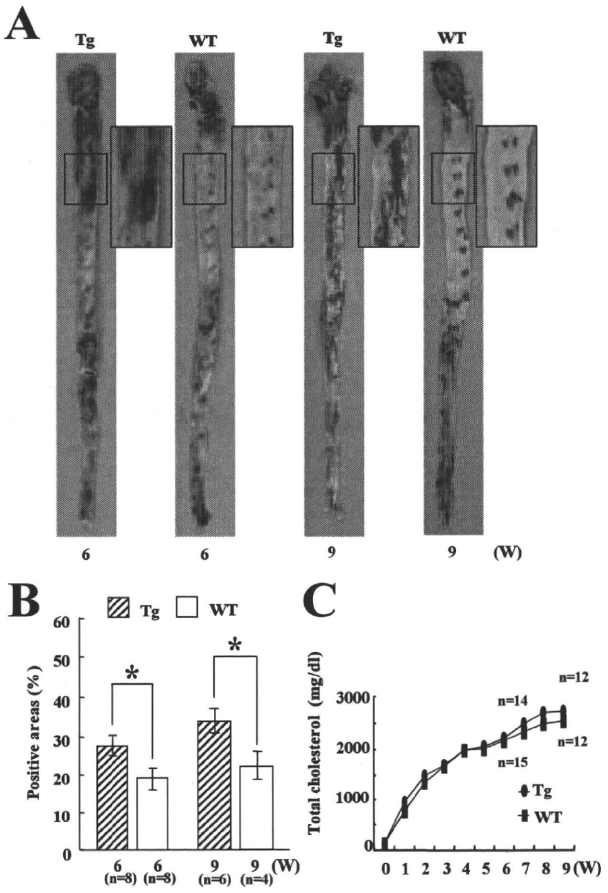

Figure 1. Quantitative analysis of gross observations of the high-cholesterol diet-induced fatty streaks. **A:** Representative oil red O-stained aortas prepared from hMMP-12 Tg and WT rabbits fed the diet containing 1% cholesterol for 6 or 9 weeks. The fatty streaks in the hMMP-12 Tg rabbits in the aortic arch and the upper portion of the thoracic aorta were grossly more extensive than those in the WT animals. Fatty streaks of WT animals were mainly located in the bronchial artery branches and in the distal portion of the intercostal artery branches, whereas fatty streaks in the hMMP-12 Tg rabbits were diffusely spread throughout the aorta. **B:** En face quantitative analysis of the oil red O-stained portion of whole aortas. Data are expressed as the mean ± SE (n, number of aortas). $^*P < 0.05$. **C:** Total cholesterol levels in hMMP-12 Tg and WT rabbits fed a diet containing 1% cholesterol up to 9 weeks are shown in the graph. Data are expressed as the mean ± SE (n, number of rabbits).

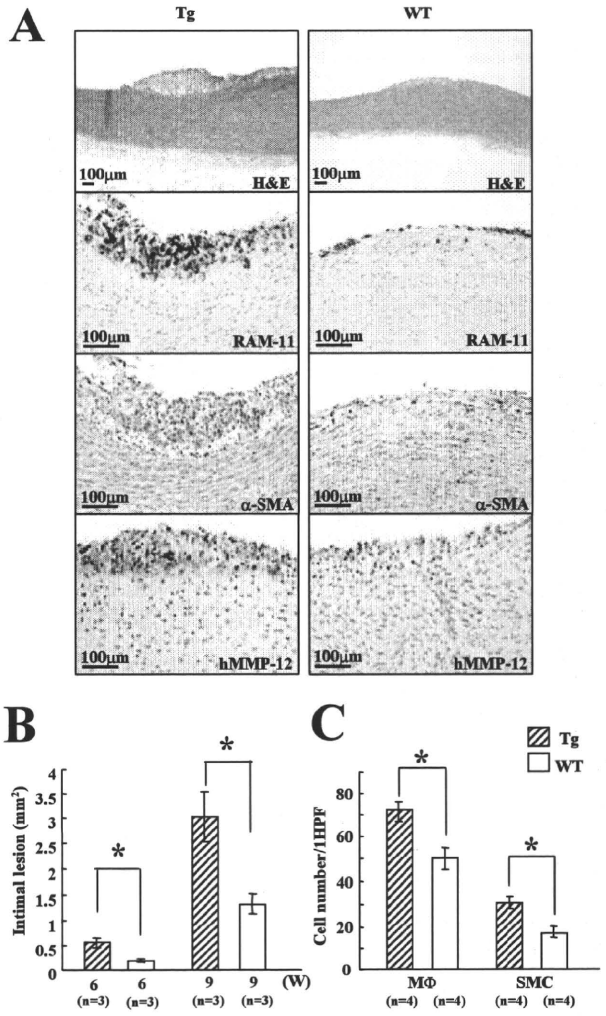

Figure 2. Quantitative analysis of microscopic observations of the high-cholesterol diet-induced fatty streaks in the aortic arch and the upper portion of the thoracic aorta. **A:** Serial paraffin cross sections of aortas stained immunohistochemically with antibodies against macrophages (RAM-11), SMCs (α-SMA), and hMMP-12. **B:** Quantitative microscopic measurements indicated that the intimal lesion area was increased about 3.0-fold (6 weeks) or 2.3-fold (9 weeks) in hMMP-12 Tg aortas compared with that for the WT aortas. Data are expressed as the mean ± SE (n, number of aortas; number of sections = 9 for Tg and WT). $^*P < 0.05$. **C:** Immunohistochemical quantification of the lesional cellular components revealed a significantly larger number of RAM-11-reactive macrophages and α-SMA-positive SMCs in hMMP-12 Tg rabbits than in the WT rabbits. Data are expressed as the mean ± SE (n, number of aortas). $^*P < 0.05$.

sis than WT rabbits, wherein a large number of RAM-11-reactive macrophages and a much smaller number of α-SMA-positive SMCs had accumulated and synthesized hMMP-12 in the fatty streaks (Figure 2A). Statistical microscopic analysis by atherosclerosis grading of the aortic arch and the upper portion of the thoracic aorta revealed that the intimal lesion area or I/M ratio was significantly increased about 2.3- to 3.0-fold in hMMP-12 Tg rabbits fed the high-cholesterol diet for 6 or 9 weeks compared with that for the WT rabbits ($P < 0.05$; Figure 2B). α-SMA-positive SMCs were also diffusely distributed in the fatty streaks, and some of these cells were located in the deep portion of the lesions close to the media. The numbers of macrophages and SMCs in fatty streaks of hMMP-12 Tg rabbits were significantly larger than those in WT animals ($P < 0.05$; Figure 2C).

Quantitative Analysis of Fatty Streaks and Elastolysis in the Distal Portion of the Thoracic Aorta

To study the relationship between fatty streaks and elastolysis of the most inner elastic layer below the endothelium, we examined fatty streaks in the thoracic aorta from hMMP-12 Tg and WT rabbits fed the 1% cholesterol diet for 6 weeks, by which time relatively slight fatty streaks had appeared, and we limited the observation area to about 10 mm in length, as shown in Figure 3A. For investigation of disruption of the elastic layers (Figure 3B), of up to 2500 serial 4-μm-thick sections, up to 250 were stained with H&E or EVG. The

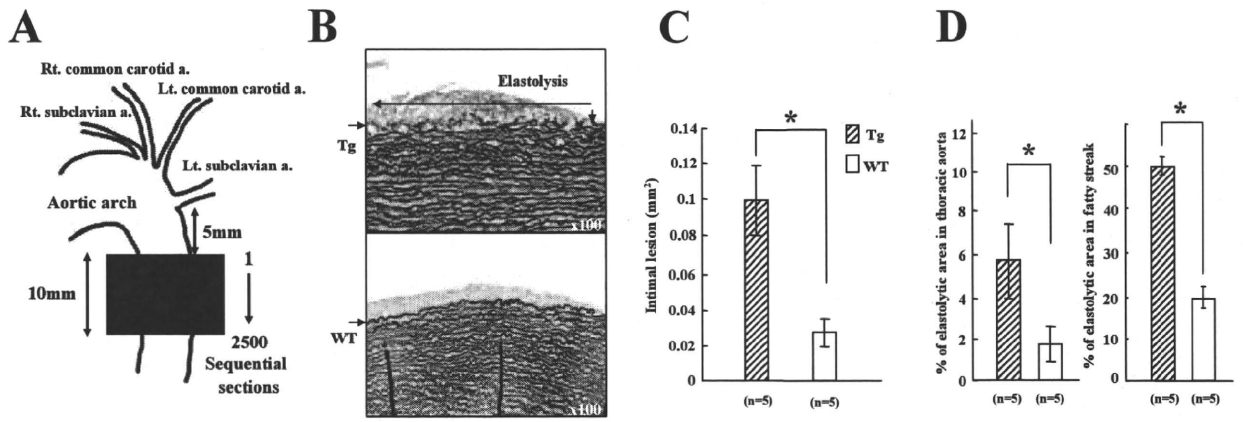

Figure 3. Quantitative microscopic analysis of the high-cholesterol diet-induced fatty streaks and elastolysis in the distal portion of the thoracic aorta. **A:** A schema for preparation of sequential sections of the intercostal artery area. **B:** Micrographs represent elastolytic portion of the internal elastic layer (**arrows**) observed in a fatty streak, particularly in EVG-stained sections of an hMMP-12 Tg rabbit. **C** and **D:** Quantitative microscopic measurements of intimal lesion area (**C**) and elastolysis ratio (**D**). The significantly increased intimal lesion area of hMMP-12 Tg rabbits was associated with approximately 3.2-fold more progressive elastolysis of the internal elastic layer compared with that for the WT rabbits. Data are expressed as the mean ± SE (n, number of aortas; total number of sections = 74 and 51 for intimal lesion area and elastolysis, respectively). $^*P < 0.05$.

quantitative analysis of the intimal lesion area for these serial sections confirmed the area to be significantly larger in hMMP-12 Tg animals ($P < 0.05$; Figure 3C) and showed approximately 2.5- to 3.2-fold more progressive elastolysis of the elastic layer in these animals than in the WT rabbits ($P < 0.05$; Figure 3D). The general relationship between fatty streaks and elastolysis is shown in Figure 4.

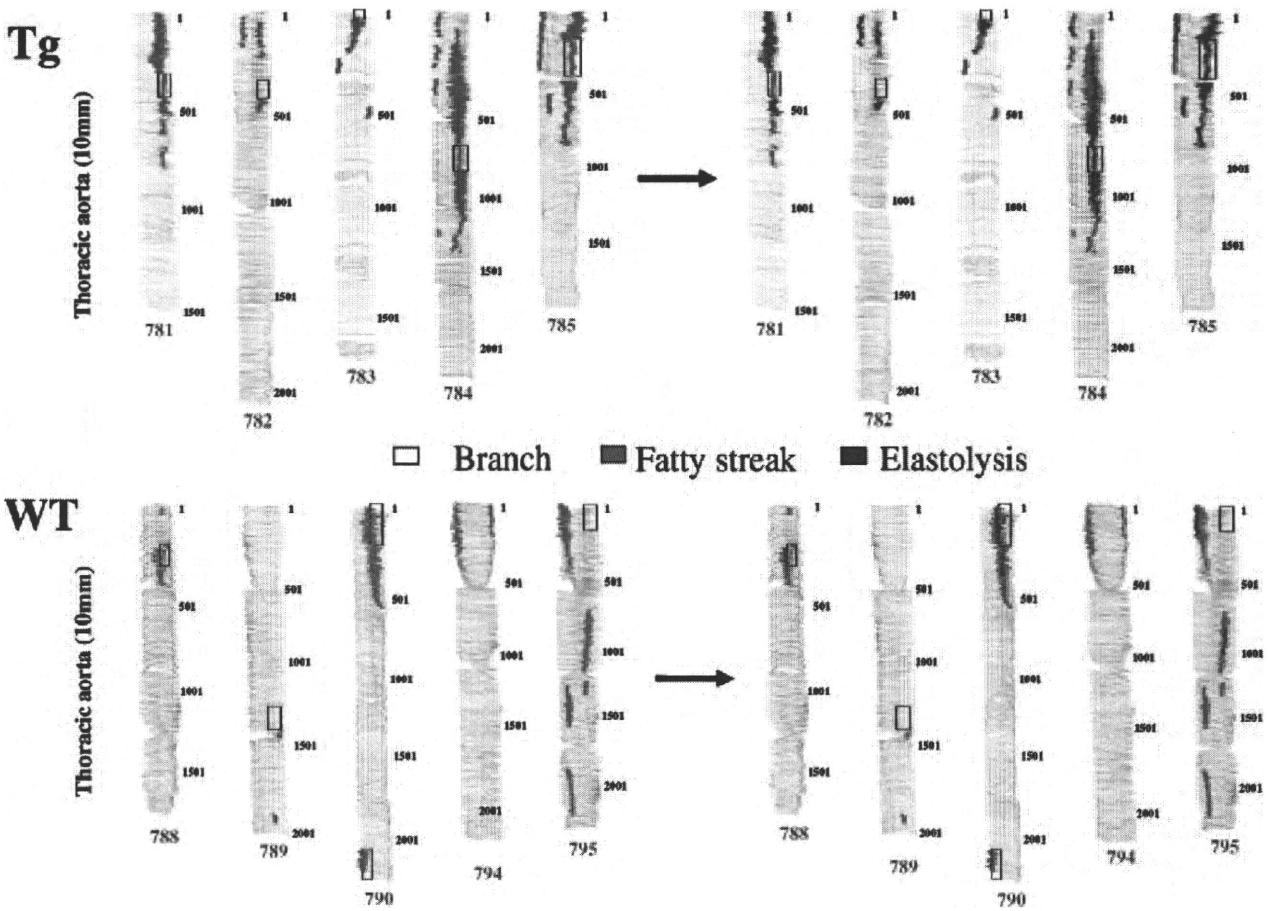

Figure 4. Scheme of relationship between fatty streaks, elastolysis, and intercostal artery branches in the thoracic aorta. Photographs show elastolytic areas (blue lines) in fatty streaks (red lines) in high-cholesterol diet-fed hMMP-12 Tg (nos. 781 to 785) and WT rabbits (nos. 788 to 790 and 794 to 795). Fatty streaks were relatively developed in relation to intercostal artery branches in WT animals, whereas in hMMP-12 Tg, the lesion was spread diffusely in the distal thoracic aorta. Elastolytic lesions were almost entirely located in fatty streaks.

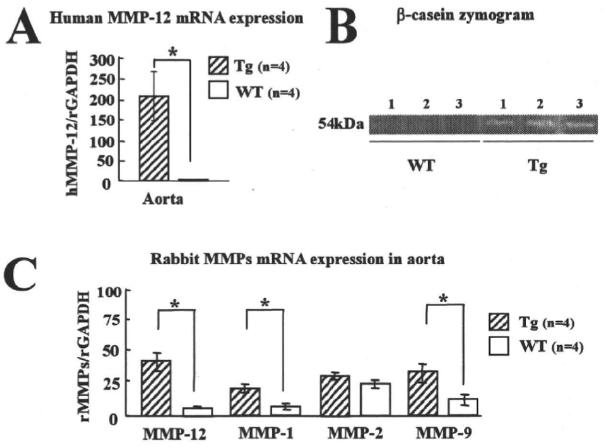

Figure 5. Real-time RT-PCR analysis and activity of hMMP-12 expression and rMMPs expression in cholesterol-induced atherosclerosis. **A:** In hMMP-12 Tg rabbits, analysis of real-time RT-PCR demonstrated the expression of hMMP-12 mRNA in atherosclerotic aortas fed a diet containing 1% cholesterol for 6 weeks but not in WT animals. Data are expressed as the mean ± SE (n, number of aortas). $^*P < 0.05$. **B:** Zymography of hypercholesterolemia-induced atherosclerotic aortas showed that clear bands of hMMP-12 (with estimated sizes of 54-kDa) in samples prepared from Tg rabbits could digest casein, indicating that these proteins were enzymatically active. No definitive bands were found in samples from non-Tg animals. **C:** Rabbit MMPs, including rMMP-1, -9, and -12, from the Tg atherosclerotic aortas were more significantly expressed than those from WT aortas. Expression levels of all MMP mRNA were normalized by those of rabbit glyceraldehyde-3-phosphate dehydrogenase mRNA. Data are expressed as the mean ± SE (n, number of aortas). $^*P < 0.05$.

Expression of hMMP-12 and rMMPs in hMMP-12 Tg Rabbits

The aortas from hMMP-12 Tg rabbits fed the 1% cholesterol diet also showed a quite increased expression of hMMP-12 mRNA, but those from WT animals did not, as evaluated by the real-time RT-PCR method (Figure 5A). In the vascular cuff and ligation models, the arteries from hMMP-12 Tg rabbits also revealed the increased expression of hMMP-12 (Figure 6A); but these levels were lower than those in the aortas of the cholesterol-fed rabbits, and those from the WT animals showed no expression of it. Zymographic assays of these aortas showed that caseinolytic activities were present in the 54-kDa band obtained with the hMMP-12 Tg hypercholesterolemia-induced atherosclerotic aortas and cuff-injured arteries were markedly increased compared with those in WT aortas (Figures 5B and 6B). These results confirmed that the atherosclerotic lesion from Tg rabbits consistently contained high levels of hMMP-12 proteins that were enzymatically active.

Additionally, except for rMMP-2, other rMMPs including rMMP-1, -9, and -12 from the Tg atherosclerotic aortas were significantly expressed more than those from WT aortas (Figure 5C) but not in the case of cuff- and ligation-induced arteries (Figure 6, C and D).

Atherosclerosis Caused by Cuff- or Ligation-Induced Injury in Muscular Arteries

For statistical analysis of cuff- or ligation-induced atherosclerosis, step or sequential sections (up to 900) were

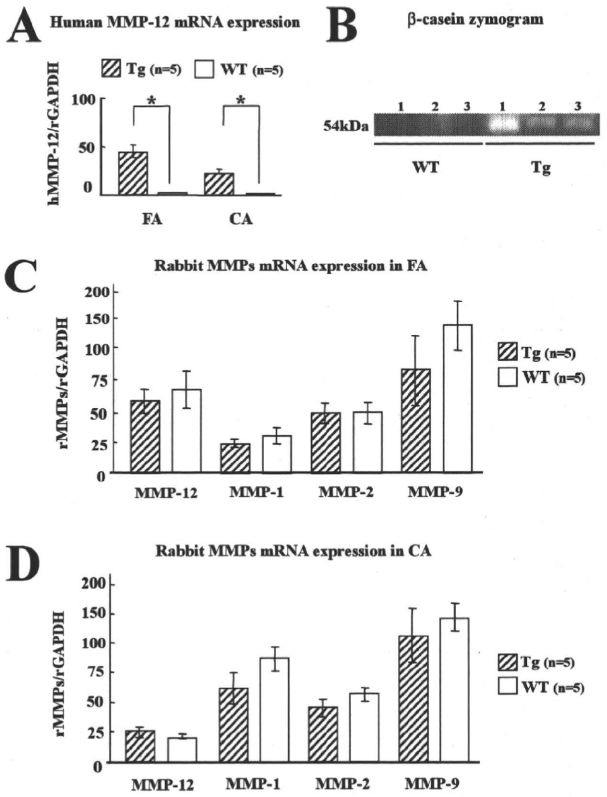

Figure 6. Real-time RT-PCR analysis and activity of hMMP-12 and rMMPs expression in cuff- and ligation-induced atherosclerosis. **A:** Analysis by real-time RT-PCR demonstrated the expression of hMMP-12 mRNA in cuff-injured femoral arteries and in ligation-injured carotid arteries after 3 weeks in hMMP-12 Tg rabbits but not in WT animals. Data are expressed as the mean ± SE (n, number of arteries). $^*P < 0.05$. **B:** Zymography shows clear proteolytic activity of hMMP-12 (with estimated sizes of 54-kDa) only from cuffed arteries of Tg rabbits, indicating the digestion of casein as seen in Figure 5. No definitive clear bands were detected in WT rabbits. **C** and **D:** Rabbit MMPs, including rMMP-1, -9, and -12, from the Tg rabbits with cuff-induced (**C**) and ligation-induced (**D**) atherosclerosis were tested by real-time RT-PCR. Unlike cholesterol-induced atherosclerosis, no significant difference in the expression of rMMPs between Tg and WT animals was detected for any of the rMMPs tested. Expression levels of all MMP mRNAs were normalized by those of rabbit glyceraldehyde-3-phosphate dehydrogenase mRNA. Data are expressed as the mean ± SE (n, number of arteries).

also prepared and used for the observation of atherosclerosis coupled with degradation of the internal elastic lamina. In histological examination coupled with immunohistochemical staining, the results demonstrated that in the cuff and ligation models, the hMMP-12 Tg rabbits 3 weeks after the surgical treatment showed significantly more atherosclerosis than the WT rabbits (Figure 7A), although there was no significant difference between hMMP-12 Tg and WT rabbits 1 week after the surgical treatment (data not shown). Determination of the I/M ratio revealed an approximate 2.3-fold (cuff model) or 2.2-fold (ligation model) greater value for the hMMP-12 Tg rabbits than for the WT rabbits ($P < 0.05$; Figure 7B).

Immunohistochemically, the neointima caused by the cuff- or ligation-induced injury was predominantly composed of SMCs positive for α-SMA and a few scattered macrophages reactive with the RAM-11 antibody (Figure 8A). In contrast, in the tunica adventitia of the cuff-injured femoral arteries, a larger number of infiltrating monocytes/macrophages was found; and their number was

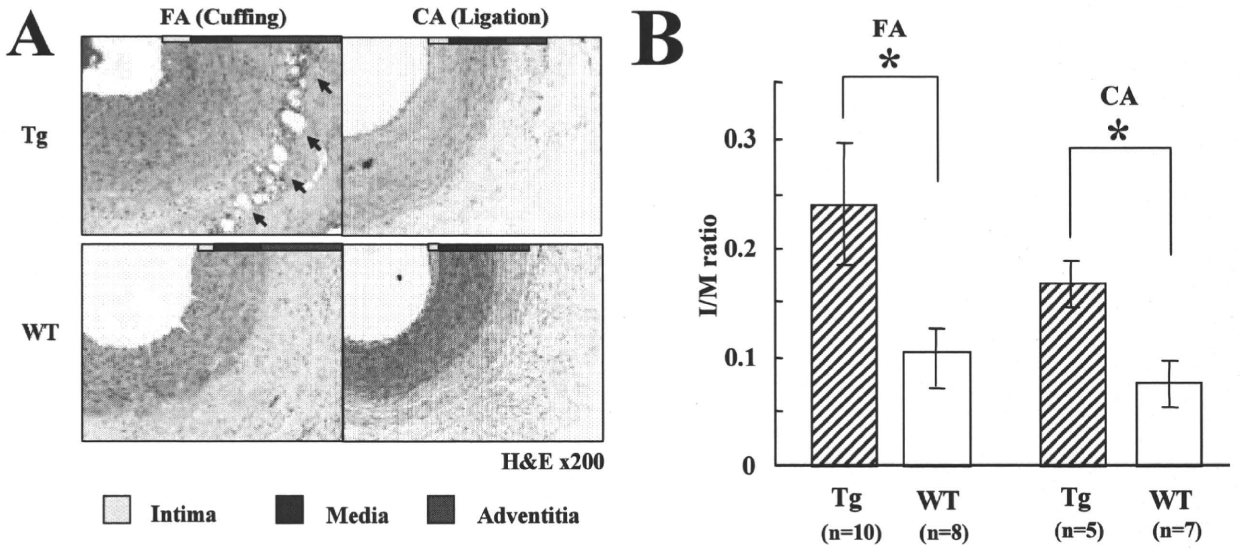

Figure 7. Microscopic observation of cuff-induced and ligation-induced atherosclerotic lesions in muscular arteries. **A:** Representative micrographs show cuffed-femoral and ligated-carotid arteries of hMMP-12 Tg and WT rabbits after 3 weeks of cuffing or ligation (H&E staining). The cuff-induced and ligation-induced intimal thickening of hMMP-12 Tg animals was greater than that of WT rabbits. In hMMP-12 Tg rabbits, inflammation in the tunica adventitia (**arrows**) was more conspicuous than that in WT rabbit. **B:** Quantitative I/M ratio was increased about 2.3- and 2.2-fold in cuff- and ligation-induced model, respectively, at 3 weeks for hMMP-12 Tg rabbits compared with that for the WT animals. Data are expressed as the mean ± SE (n, number of arteries; number of sections = 11–17 for artery). $^*P < 0.05$.

greater in the hMMP-12 Tg than in the WT rabbits (Figure 8A, left middle row). hMMP-12-positive cells in the tunica adventitia appeared to overlap with these macrophages only in the cuff-injured hMMP-12 Tg animals (Figure 8A, left bottom row). The number of infiltrating macrophages in the tunica adventitia of the cuffed hMMP-12 Tg rabbits was about 2.2-fold larger than that for the WT rabbits ($P <$ 0.05; Figure 8B). In the ligation model, except for the ligation site with foreign body-type inflammation caused by the suture, adventitial inflammation was extremely weak compared with that in the cuff-injury model (Figure 8A, right); and there was no significant difference between hMMP-12 Tg and WT rabbits 1 or 3 weeks after the surgical treatment (data not shown).

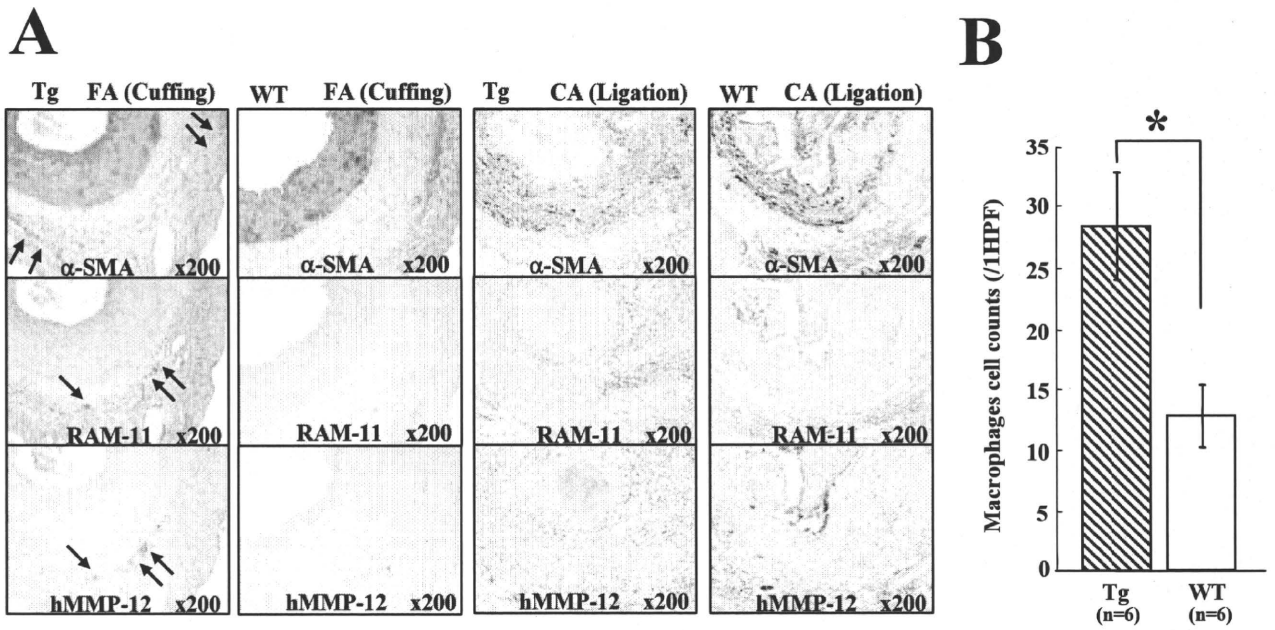

Figure 8. Immunohistological observation of cuff-induced and ligation-induced atherosclerotic lesions in muscular arteries. **A:** Immunohistochemical staining revealed the neointima to be composed predominantly of SMCs positive for α-SMA and a few macrophages reactive with RAM-11. In the tunica adventitia of the hMMP-12 Tg rabbits, a relatively larger number of macrophages (**arrows**) and SMCs (**arrows**) had infiltrated than in the case of that of the WT animals. Additionally, a number of hMMP-12-positive inflammatory cells (**arrows**) appeared to overlap with these RAM-11-reactive macrophages but only in the cuff-injured hMMP-12 Tg rabbits. In the ligation model, near the ligation site but not in other areas, foreign body-type inflammation was recognized. **B:** In the tunica adventitia, the number of macrophages in cuff-injured hMMP-12 Tg rabbits was about 2.2-fold larger than that for the WT animals. Data are expressed as the mean ± SE (n, number of arteries). $^*P < 0.05$.

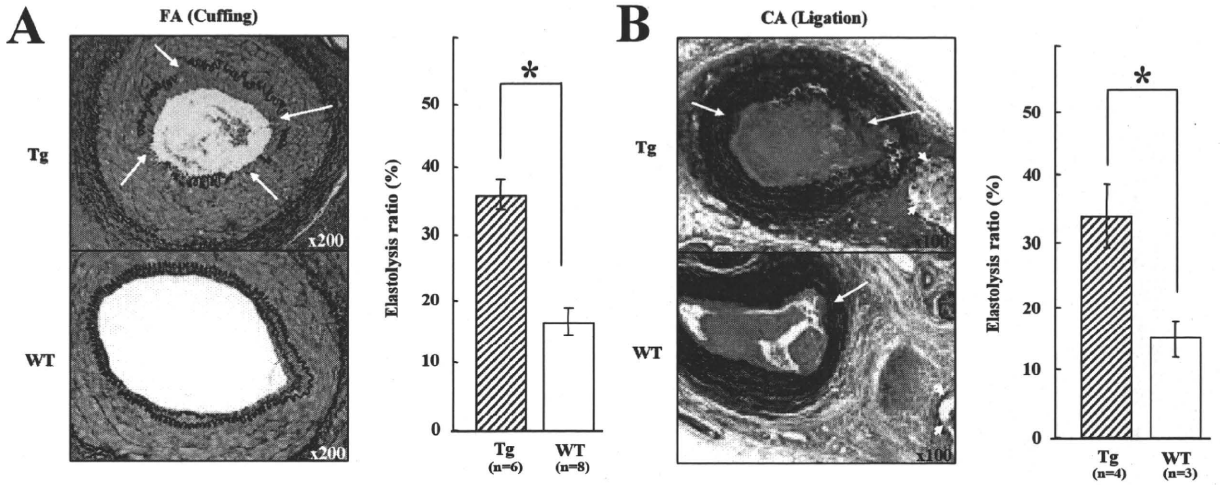

Figure 9. Quantitative analysis of elastolysis of cuff-induced and ligation-induced atherosclerotic lesions in muscular arteries. **A:** Elastolytic lesions (**white arrows**) in cuffed femoral arteries after 3 weeks. The elastolytic ratio was significantly greater for cuff-injured hMMP-12 Tg than for WT rabbits. Data are expressed as the mean ± SE (n, number of arteries; total number of sections = 45 and 33 for Tg and WT, respectively). $^*P < 0.05$ (EVG staining). **B:** Elastolytic activity (**white arrows**) in ligated carotid arteries after 3 weeks. Elastolytic activity in the internal elastic lamina was detected in the vessel wall just proximal to the ligation site, where foreign body-type inflammation caused by the suture (**arrowheads**) was prominent; and the elastolysis was more conspicuous in hMMP-12 Tg rabbits than in the WT rabbits. Data are expressed as the mean ± SE (n, number of arteries; total number of sections = 17 and 12 for Tg and WT, respectively). $^*P < 0.05$ (EVG staining).

Quantitative analysis of elastolysis at the internal elastic lamina showed that the elastolysis ratio was more significantly pronounced, about 2.2-fold, in hMMP-12 Tg than in WT rabbits in both models (Figure 9, A and B). The elastolysis in the carotid arteries, however, was relatively less than that in the femoral arteries and was limited to just the portion close to the ligation site with foreign body-type inflammation (Figure 9B).

Another type of elastolysis was found at 1 and 3 weeks but only in the cuff model. In particular, 1 week after the surgical treatment, "microelastolytic points" were recognized in the nonatherosclerotic portions before formation of the neointima (Figure 10). Immunohistochemically identified SMCs seemed to be associated with these microelastolytic points (not shown). There was no significant difference in the number of these points between hMMP-12 Tg and WT rabbits at 1 or 3 weeks after the surgical treatment (data not shown).

Discussion

In our previous study on atherosclerosis induced in hMMP-12 Tg rabbits consuming a diet including 0.2% cholesterol for 16 weeks, there was no significant difference in the early stage of atherosclerosis between hMMP-12 Tg and WT "lower hypercholesterolemia" animals.[23] Considering the actions of hMMP-12 in advanced atherosclerosis, these data were unexpected. The hMMP-12 transgene was under the control of the human scavenger receptor-A enhancer/promoter, which is not the promoter for the MMP-12 gene, as a macrophage-specific promoter[21,26] in hMMP-12 Tg animals. The hMMP-12 Tg rabbits were generated to investigate pathological events in relation to atherosclerosis under overexpression of MMP-12. Therefore, in current study, we studied pronounced fatty streaks composed of larger number of foam cells under the condition of a higher serum cholesterol than was present in the previous study. The current data reveal a significant role of hMMP-12 even in the formation of early atherosclerotic lesions.

The quantitative analysis of fatty streaks in en face (Figure 1) showed that the early atherosclerotic lesions in whole aortas of the Tg rabbits were significantly more progressive than those of the WT rabbits, indicating that a larger number of monocytes/macrophages had migrated from the peripheral blood to the intima to phagocytose lipid in the former animals. The analysis of cut sections in aortic arches, the upper portion of the thoracic aorta, and the distal portion of the intercostal artery branches arising from the thoracic aorta also revealed significantly more pronounced lesions in terms of the intimal area and showed immunohistochemically that a larger number of monocytes/macrophages had infiltrated in hMMP-12 Tg than in WT rabbits (Figure 2). These results strongly suggest that hMMP-12 expression accelerated the migration of monocytes/macrophages into the intima by basement membrane proteolysis.

Currently, it is thought that lipid deposition is a necessary but not sufficient condition for the development of human atherosclerosis. Because elastin is a critical matrix component of the artery not only to maintain its elastic nature but also to divide structurally the intima from the media, disruption of the elastic fibers by MMP-12 within fatty streaks could cause a morphologically minor but critical microenvironmental change affecting SMCs in the media. Therefore, the quantitative analysis of elastolysis associated with fatty streaks was performed by examining sequential sections of the lower portion of the thoracic aorta from rabbits fed the high-cholesterol diet for 6 weeks, at the end of which time, the extremely early fatty streaks have appeared. The results showed that disruption of the internal elastic layer in hMMP-12 Tg rabbits was also significantly increased compared with that in